University of Nevada, Reno

Using an Integrated Model to Assess Groundwater Recharge in Martis Valley, CA

A thesis submitted in partial fulfillment of the requirements for the degree of Master of Science in Hydrogeology

by

Murphy A. Gardner

Dr. Greg Pohll – Thesis Advisor

May 2014

UNIVERSITY OF NEVADA RENO

THE GRADUATE SCHOOL

We recommend that the thesis
prepared under our supervision by

Murphy A. Gardner

entitled

Using an Integrated Model to Assess Groundwater Recharge in Martis Valley, CA

be accepted in partial fulfillment of the
requirements for the degree of

MASTER OF SCIENCE

Greg Pohll, Ph.D., Advisor

Matt Reeves, Ph.D., Committee Member

Simon Poulson, Ph.D., Committee Member

Justin Huntington, Ph.D., Graduate School Representative

Marsha H. Read, Ph.D., Dean, Graduate School

May, 2014

Abstract

Groundwater contributes an essential water supply to several communities and ecosystems in the Truckee River Basin. Water resource investigations were conducted through numerical modeling and comparisons to previous work to assess groundwater recharge in the Martis Valley watershed, which is an essential component to the Truckee River hydrographic region. A baseflow analysis was performed to relate annual baseflow to streamflow and precipitation. Results show that changes in groundwater fluctuations are driven by changes in precipitation, and baseflow response is affected by previous precipitation trends. It was estimated that baseflow is roughly one-sixth of mean annual precipitation. A novel method for constructing a hydrogeologic framework model was developed and applied to an integrated surface water-groundwater hydrologic model, GSFLOW, from which groundwater recharge locations and magnitudes were extracted. Model results supplemented previous work and provided enhanced conceptualizations of surface and groundwater interactions, as well as spatial and temporal recharge trends. Results show that the most significant recharge zones are low to mid-elevation stream channel and alluvial areas. During peak snowmelt periods, upper elevation alluvial areas also contribute significant recharge. The findings herein promote a more detailed understanding of groundwater recharge characteristics in high elevation, snow dependent, alpine catchments.

Acknowledgements

Funding that for this research was provided by the U.S. Department of the Interior, Bureau of Reclamation. This thesis research was made possible largely by the fellow researchers who walked me through uncertain areas of my project, kept ideas flowing, and contributed an immense amount of time and knowledge. I owe gratitude to my advisor, Greg Pohll, who provided the opportunity for this research, as well as sincere guidance and consistent leadership throughout my thesis research and other projects that I was involved with. Justin Huntington and Matt Reeves were immensely helpful in both developing the hydrologic model and structuring my thesis. Rich Niswonger and Charles Morton provided much needed assistance when troubleshooting modeling issues and extracting results. All aforementioned parties were major contributors to the hydrologic model used for this research, and took time out of their busy schedules to help with my thesis. Simon Poulson provided professional critiques that helped organize and clarify my work, as well as present the geochemical aspects in a reasonable way. I want to thank Ron Hershey for taking time to discuss the geochemical data, and point me in the right direction. Daniel Segal of California State University East Bay along with Jean Moran and Mike Singleton of Lawrence Livermore National Laboratory graciously shared geochemical data and interpretations from Segal's master's thesis work, which gave this research a unique edge. Lisa Wable designed the appealing conceptual model illustration based off a much less appealing hand drawn sketch. Apart from the academic support, I have been blessed with incredible friends and family whose endless support has allowed me to take full advantage of great opportunities.

Table of Contents

List of Tables

List of Figures

Introduction

The Truckee River watershed receives a significant portion of its water supply from Lake Tahoe outflow and surface and groundwater contributions from the Martis Valley basin. Interconnected surface water and groundwater (SW/GW) systems are complex and require integrative investigations to understand governing hydrologic processes. Understanding and quantifying interactions between SW/GW on a spatial and temporal level is highly desirable, but their co-varying nature makes this difficult at the watershed scale. One process that governs SW/GW interactions is groundwater recharge. Groundwater recharge is defined as the infiltration of water beyond the root or soil zone that reaches the water table (Healy, 2010). In the Great Basin, mountain front recharge is a large component of total recharge, but physical and climatic heterogeneity within and between basins makes recharge estimations site-specific and highly variable on an annual time scale. Measurements of recharge can provide local information, but obtaining direct measurements of basin-scale groundwater recharge is beyond the scope of current technology. Previous recharge studies in Martis Valley have employed water budget estimation techniques and geochemical analyses. Model simulations can provide important insight into the functioning of hydrologic systems by identifying factors that influence recharge (Healy, 2010). Integrated models simulate interconnected hydrologic processes and facilitate the understanding of watershed-scale trends and relationships.

This research focused on investigating groundwater recharge location, timing, and magnitude in the Martis Valley watershed. A baseflow analysis provided preliminary insight into the relationships between precipitation, runoff, baseflow, and their relation to recharge. An integrated groundwater-surface water model, GSFLOW, was used to assess

the spatial and temporal distribution of groundwater recharge throughout the Martis watershed, and estimate mean annual recharge volumes at basin and sub-basin scales. Recharge occurs along the entire elevation profile of Martis Valley, however, specific areas of concentrated recharge in Martis Valley remain an open research question. Maxey-Eakin based estimates generally assign recharge to the upper elevations where the majority of precipitation falls, while the geochemical investigations reviewed in this report suggest an opposite spatial trend. Annual recharge magnitudes were simulated in the GSFLOW model as a function of the climatic model drivers, precipitation and temperature, as well as hydrogeologic parameters assigned throughout the watershed. Results from GSFLOW were compared to previous recharge estimates and geochemical interpretations.

Martis Valley Watershed

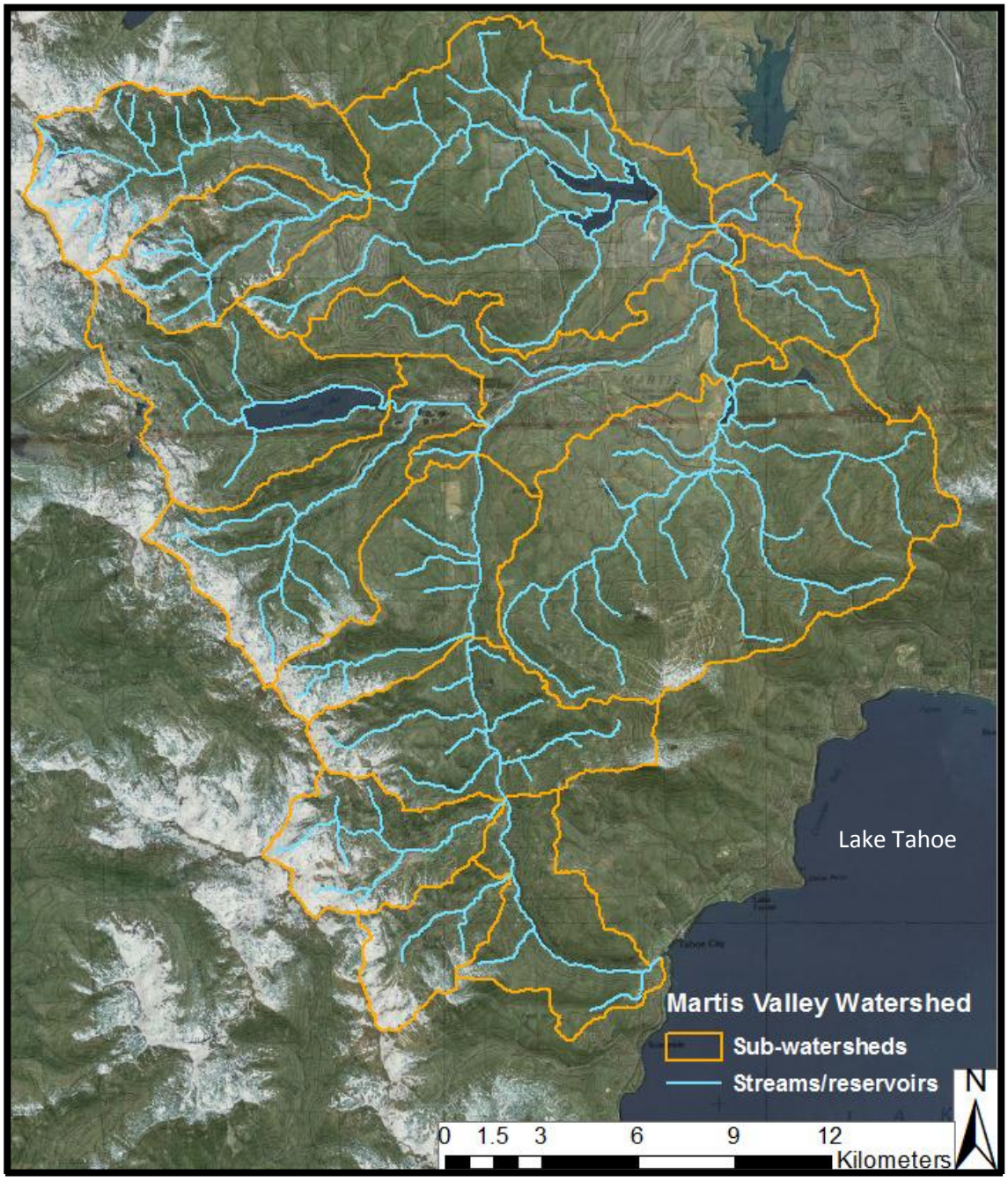

Figure 1: The Martis Valley watershed and sub-basins. The watershed border runs northwest along the Sierra Nevada crest, then eastward to capture the northern sub-watersheds that drain into Prosser Creek Reservoir, and finally south and west along the ridgeline made up of Martis Peak, Brockway Summit, and Mt. Pluto, before returning to the Truckee River discharging from Lake Tahoe at Tahoe City.

Previous Work

Numerous methodologies have been developed to estimate groundwater recharge over various spatiotemporal scales. As previously stated, recharge at a basin-wide scale is difficult to estimate and nearly impossible to directly measure; therefore, hydrologists have typically relied on indirect estimation techniques. Some commonly used techniques include physical and empirical methods, environmental tracers, and numerical models (Carling et al., 2012). Since the 1950s, recharge estimations in the Great Basin have largely been based off the empirical relationship developed by Maxey and Eakin (1949) that relates groundwater recharge to mean annual precipitation. This technique and its modified versions (Nichols, 2000; Epstein et al., 2010) estimate recharge by applying recharge coefficients to precipitation amounts. This section focuses on previous groundwater recharge investigations of Martis Valley and similar watersheds that used water budget, geochemical, numerical modeling, and baseflow analysis methods.

Water Budgets

In Martis Valley, past recharge estimations have relied on empirical and water balance methods. Hydro-Search, Inc. (1974) performed the first comprehensive recharge study, which was updated in 1980 and again in 1995 as part of the Martis Valley Groundwater Management Plan prepared for Truckee Donner Public Utility District (TDPUD). Hydro-Search, Inc. (HSI) used a water budget approach to calculate available water within the Martis Valley Groundwater Basin (MVGB), a subset of the Martis Valley hydrographic area, delineated in the 1974 HSI study. To estimate recharge, HSI

sectioned the MVGB into 10 zones assumed to contain homogenous hydrologic properties. Recharge was estimated for each zone using an approximation method based on infiltration characteristics of the soil and geologic formations, evapotranspiration (ET) losses, depth to groundwater, and precipitation amount. These categories were rated based on their recharge capabilities, and a percentage of precipitation termed "recharge efficiency" (12.5% - 27%) was assigned to each zone based on these ratings. Total recharge estimated by HSI within the MVGB was approximately 18,179 acre-feet per year (ac-ft/yr). Nimbus Engineers (2001) used the same basin delineations as HSI and used the HSI recharge estimations as a framework for their study. Recharge efficiencies were assigned to the ten zones from the HSI report based on slope, aspect, soil, and geologic unit. Parameter-elevation Regressions on Independent Slopes Model (PRISM) simulated precipitation data were used, resulting in an additional 6,320 ac-ft/yr of precipitation to the MVGB compared to the HSI precipitation data. The Nimbus Engineers (2001) report concluded that the basin-wide recharge efficiency is 25.3% and annual recharge is 23,744 ac-ft/yr. Kennedy/Jenks Consultants (2001) published an independent assessment of Martis Valley groundwater availability suggesting that the earlier studies by HSI (1974, 1980, 1995) and Nimbus Engineers (2001) were conservative resulting from the under prediction of groundwater discharge to streams, but no recharge estimations were provided in this report. InterFlow Hydrology, Inc. and Cordilleran Hydrology, Inc. (2003) presented measurements of groundwater discharge to Truckee River tributary streams in Martis Valley. This report suggested that recharge had been underestimated in previous studies due to limited discharge data and the omission of certain watershed areas that contribute to recharge. The study focused on

data collection in tributary streams to refine the previous investigations. Streamflow measurements showed a total of 34,560 ac-ft/yr of groundwater discharge to streams tributary to the Truckee River, of which approximately 24,240 ac-ft/yr is contributed by high elevation areas, while the remaining 10, 320 ac-ft/yr occurs in lower elevations within the MVGB. Rajagopal et al. (2012) applied the Precipitation Runoff Modeling System (PRMS) to estimate recharge in Martis Valley. The PRMS simulated recharge varies from year to year based on precipitation and temperature cycles. The average annual recharge estimate for a 30 year historical period was 32,745 ac-ft/yr. In the same report, a modified Maxey-Eakin method was described and resulted in an estimate of 35,168 ac-ft/yr of groundwater recharge. Because the numerical model is surface water focused, the influence of low permeability mountain block in rejecting infiltrating water is neglected; therefore the spatial distribution of recharge was largely driven by precipitation location. Recharge locations can be simulated more realistically by integrated surface water-groundwater modeling and inferred from isotope and dissolved gas measurements. Table 1 presents a summary of previous water budget-based groundwater recharge estimations for Martis Valley.

Summary of GW Recharge Estimations in Martis Valley	
Hydrosearch, Inc (1995)	18,179 ac-ft/yr
Nimbus Engineers (2001)	23,744 ac-ft/yr
Interflow Hydrology and Cordilleran Hydrology, Inc (2003)	34,560 ac-ft/yr
Seshadri et al. PRMS (2012)	32,745 ac-ft/yr
Seshadri et al. Modified Maxey-Eaken (2012)	35,168 ac-ft/yr

Table 1: Previous estimates of groundwater recharge in Martis Valley groundwater basin.

Geochemistry

Chemical concentrations and tracers in certain contexts can be used to investigate SW/GW interactions, provide quantitative or qualitative estimates of recharge, and identify sources and locations of recharge (Healy, 2010). Observations made by Craig (1961) of isotopic values related to their sources (i.e. warm or cold regions) have become the basis for isotopic investigations of recharge. Measurements of stable isotopes deuterium (δ^2H) and oxygen-18 ($\delta^{18}O$) provide a tool for characterizing groundwater recharge environments (Clark and Fritz, 1997). Initial isotopic signatures are contained in precipitation and allude to temperature at time of deposition, therefore allowing for hydrograph separations and recharge source implications. Several studies have employed environmental isotopic analyses to investigate groundwater recharge and discharge and the components of streamflow (Fritz et al., 1976; Sklash and Farvolden, 1979; Rodhe,

1984; Kennedy et al., 1986; Bottomley et al., 1986; Herrmann et al., 1986; Turner et al., 1987). Sklash and Farvolden (1979) presented isotopic-based hydrograph separation designating groundwater dominance in storm runoff. Rhode (1984) studied the relative contribution of event water and groundwater to streamflow in several watersheds throughout Sweden. Mixing models based on these isotopic studies categorize streamflow into four components: direct deposition on the water channel, overland flow, groundwater discharge, and subsurface stormflow, or interflow (Fritz et al., 1976). Friedman and Smith (1970) studied deuterium variations in Sierra Nevada precipitation to characterize annual winter climate. Stable isotope research has been applied in snow dependent regions to investigate mechanisms, timing, and locations of recharge (Ajami et al., 2011; Druhan et al., 2004; Shanley et al., 1995).

Because baseflow is largely derived from groundwater, stream samples collected near the mountain block during baseflow conditions should provide approximate isotope values for mountain block recharge. Thiros and Manning (2001) used stable isotopes and dissolved noble gases to differentiate between valley and mountain block recharge in Salt Lake Valley, Utah. Based on isotopic values and recharge temperatures calculated from noble gas measurements, the research suggested that the Salt Lake Valley aquifer receives significant mountain-block recharge. The combination of recharge temperatures and isotopic ratios allowed Thiros and Manning (2001) to designate two zones of high recharge proportions on the east side of the Salt Lake Valley. Ajami et al. (2011) employed an isotopic data-driven method to quantify mountain block recharge rates using a recession flow analysis in an Arizona basin. This research focused on understanding recharge dynamics in mountainous catchments in relation to precipitation seasonality and

catchment storage characteristics. Ajami et al. (2011) concluded that winter frontal storms provide 50% of annual precipitation, and during dry periods, streamflow is mostly derived from groundwater stored in fractured bedrock, which has an isotopic signature indicative of winter precipitation. Wahi et al. (2008) used stable isotopes δ^2H and $\delta^{18}O$ to investigate recharge seasonality in the Upper San Pedro Basin, Arizona. The research suggested that, although over half the annual precipitation falls in the summer, recharge is dominated by winter precipitation. High summertime evapotranspiration (ET) rates and periodic snowmelt that sustains infiltration through the winter were the designated causes for wintertime recharge dominance. Uncertainties in isotopic analyses arise from spatial and temporal variability, mixing of new and old water, and isotopic fractionation processes.

Dissolved gases within the hydrologic system are well suited to examine recharge processes and groundwater transport in alpine basins (Singleton 2009). Rademacher et al. (2001) and (2005) studied chemical and isotopic fluctuations in the Sagehen watershed, just north of Martis Valley, to investigate the chemical evolution of groundwater and temporal fluctuations on stream hydrochemistry. Conclusions suggested a mean groundwater residence time of over 15 years, but significant groundwater-surface water mixing dynamics on a seasonal scale. Noble gases (He, Ne, Ar, Kr, and Xe) dissolved in groundwater can be used to supplement isotopic implications and constrain recharge elevations and rates. Noble gas solubility depends on temperature and pressure, and the conservative nature of the gases allows for estimations of water table temperatures at the time of groundwater recharge. Therefore, concentrations of the dissolved noble gases can allude to recharge locations. Manning

and Solomon (2003) derived maximum and minimum recharge temperatures based on concentrations of Ne, Ar, Kr, and N_2 in spring waters and well samples applied with a maximum and minimum elevation above mean sea level. These methods constrained a zone for potential subsurface inflow. Manning and Caine (2007) used groundwater noble gas and temperature data in an alpine watershed in Colorado to map the groundwater circulation to a maximum depth of 200 m.

Noble gas concentrations in groundwater are commonly above equilibrium solubility, thus, the amount of additional entrained gas in excess of equilibrium solubility, known as 'excess air', can be measured. Excess air amounts are related to infiltration rates and/or water table fluctuations. In the Colorado watershed studied by Manning and Caine (2007), high excess air measurements indicated large seasonal fluctuations in the water table. Apparent groundwater ages from $^3H/^3He$ data supported and further constrained the noble gas implications. These analysis techniques aided Manning and Caine (2007) in the development of a conceptual model of the complex hydrogeologic system.

Singleton and Moran (2010) conducted a detailed geochemical investigation in Squaw Valley, a sub-basin within the Martis Valley watershed. Based on noble gas concentrations and isotopic signatures measured from wells and surface water, three main contributions to groundwater flow were suggested: seasonal (shallow) recharge, older (deeper) groundwater, and upwelling magmatic fluids. Nearly all of the samples in this study contained detectable amounts of tritium (^3H), reflecting the presence of groundwater less than 50 years old. Their research also pointed to the presence of radiogenic and magmatic helium as indicators of old (>50 yrs) groundwater contribution.

Based on these relative age indicators, Singleton and Moran (2010) were able to construct a conceptualization of groundwater movement and mixing through the system. Singleton and Moran (2010) compared Squaw Valley excess air values to over 800 samples from major groundwater basins in California measured by Cey et al. (2008). Higher excess air concentrations are expected in samples containing water that recharged at high rates through bedrock fractures, or has been exposed to drastic water table fluctuations. The Squaw samples fell into the bottom tier of excess air values, indicating negligible recharge through fractured bedrock. The research also mentioned that two wells drilled horizontally into bedrock in Squaw Valley had similar excess air concentrations to those of which were measured from wells lower in the basin. This suggests that even at higher elevations, shallow recharge occurs slowly in areas where soils cover the competent bedrock, maintaining low excess air values. The results implied that the majority of groundwater recharge occurs at or below the mountain front, which was presented as evidence for the basin to be sensitive to climate change. Groundwater ages from this work suggest that the top 10-40 m of the valley groundwater aquifer is derived from infiltration of snowmelt. Once the snowmelt surge has passed and groundwater levels drop, production wells begin to draw into older water, which Singleton and Moran (2010) predicted would occur sooner in the year resulting from a reduced seasonal duration of snowpack accumulation and magnitude under future climatic conditions.

The Martis Creek sub-basin of the Martis watershed has been investigated recently using geochemical techniques. Daniel Segal, a recent graduate student at the California State University East Bay and Lawrence Livermore National Laboratory (LLNL) under Jean Moran, is currently in the process of publishing his master's thesis

work, which focused on using geochemical data to evaluate recharge processes in Martis Valley and sensitivity of the watershed to climate change. His work is referenced in the following sections. Because of similar research goals, LLNL partnered with Desert Research Institute (DRI) in order to share and compare data analyses and model results of Maris Valley research. Raw stable isotope data sampled throughout 2012 was shared by LLNL, as well as noble gas and excess air measurements along with analysis and interpretations by Segal (2013). A meeting and series of written communications took place to share research and conceptual models of the basin. The stable isotope data from LLNL contained deuterium (δ^2H) and oxygen-18 ($\delta^{18}O$) measurements from groundwater, surface water, and snow samples throughout 2012. The samples were gathered by both LLNL and DRI researchers, and laboratory measurements of δ^2H and $\delta^{18}O$ were conducted at LLNL.

As previously explained, noble gas concentrations imply temperatures and climate characteristics at the time of recharge. Recharge temperatures were calculated by LLNL from water samples taken seasonally through 2012 from ten production wells, two irrigation wells and test holes, and three springs in Martis Valley proper, located in the Martis Creek sub-basin and the sub-basin directly to the north. To compute recharge temperatures, the measured noble gas concentrations were fit to three fractionation models (partial re-equilibration, closed equilibrium, and unfractionated). Temperatures from the model with the highest χ^2 probability were chosen (Segal, 2013). These derived recharge temperatures were then compared to mean annual air temperatures at sample locations to estimate recharge elevations.

Super-saturated noble gases (notably Ne) dissolved in groundwater provide an excess air reading that can suggest rates of infiltrating water (Singleton and Moran, 2010). In other words, entrainment of air bubbles during unsaturated zone infiltration followed by dissolution in the groundwater and conservative transportation can lead to measurable concentrations of excess air. A common way to represent the amount of excess air is percent excess Ne (ΔNe) relative to the equilibrium component. From these measurements, deductions can be made about specific transport characteristics, such as unsaturated zone flow or fracture flow, as well as relative recharge rates and temperatures (Singleton and Moran, 2010). In Martis Valley, excess air research was undertaken by LLNL to investigate spatial distribution of groundwater recharge. The same excess air values (from Cey et al. 2008) used for comparison in Squaw Valley by Singleton and Moran (2010) were used as reference for the Martis Valley excess air measurements.

Calculated recharge temperatures from LLNL were found to be generally within the range of mean annual air temperature (MAAT) for the elevation of sample location, therefore implying infiltration through a soil zone that sustains MAAT, rather than direct snowmelt infiltration to the water table (i.e. fracture flow). This is interpreted as more recharge occurring through alluvial formations in the lower elevations compared to direct snowmelt infiltration at higher elevations (Segal, 2013). A general trend of lower recharge temperatures with increasing elevation is suggested (Figure 2 and 3). Relatively high recharge temperatures compared to mean annual air temperatures at the sample elevation indicate higher recharge at lower elevations.

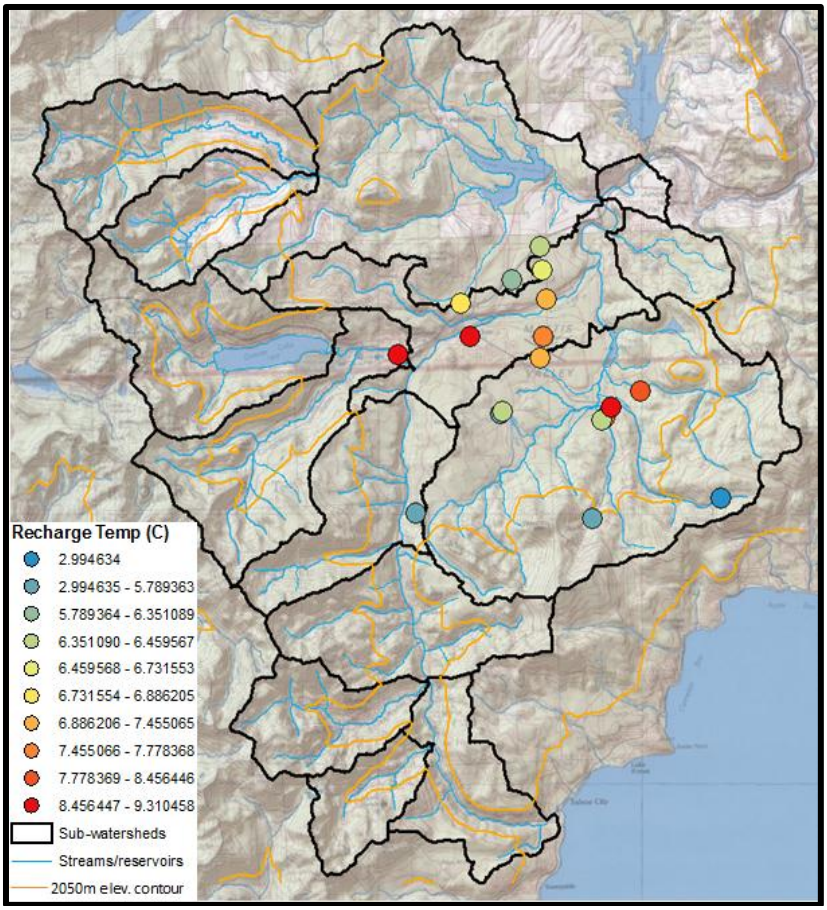

Figure 2: Noble gas recharge temperatures are similar to MAAT at the sample location, indicating recharge below the 2050 m elevation line (the lower 330 m of the watershed), where infiltrating water equilibrates with air temperature and is reflected in the noble gas concentration of the water sample.

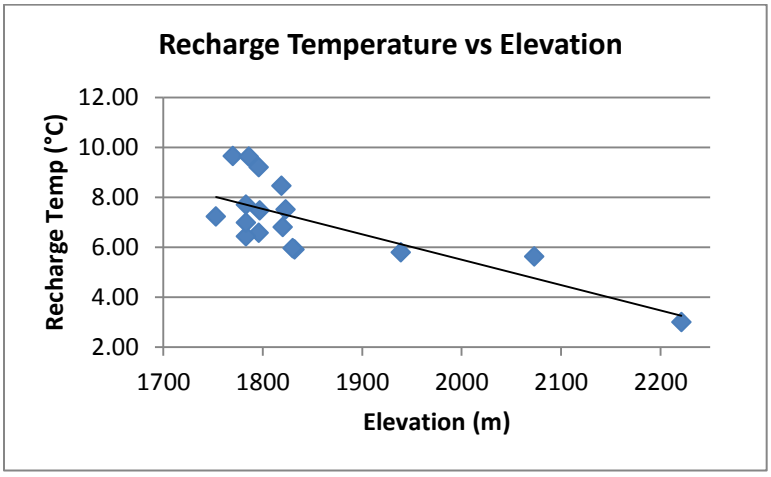

Figure 3: Decreasing trend of recharge temperature with increasing elevation.

The relatively low excess air values (compared to Cey et al., 2008) from groundwater and surface water samples in Martis Valley indicate slower infiltration rates, likely through alluvial soils in the unsaturated zone along the valley floor (Segal, 2013). Figure 4 shows the excess air values at the sample locations.

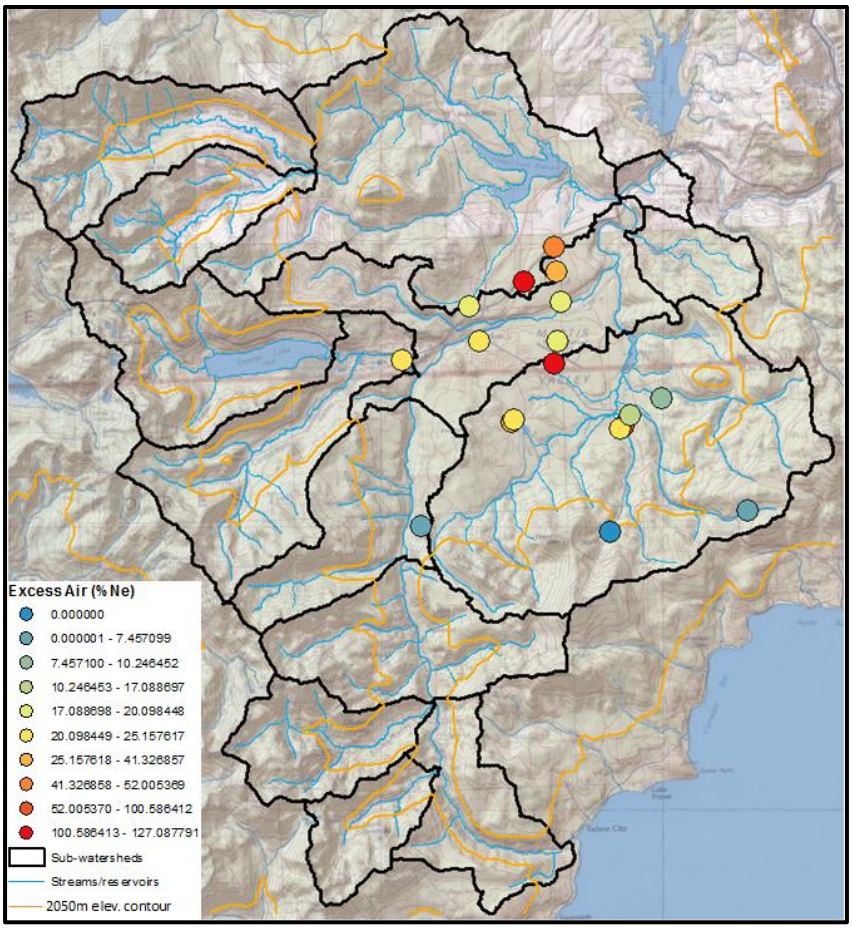

Figure 4: Excess air values (measured in %Ne excess of solubility) throughout Martis Valley fall in the mid to low range compared to measurements from around California sampled under the GAMA program (Cey et al., 2008). The relatively low values indicate dominance of slow infiltration through a soil zone (Segal, 2013). Some higher values within the valley suggest more rapid recharge rates, or larger water table fluctuations.

The excess air values are indicative of low recharge rates in upper elevations of the watershed, suggesting most recharge occurs within lower elevations. Because excess air measurements indicate conditions under which recharge occurred, high levels can be associated with mountain block recharge in the form of fracture flow. Lower levels of excess air are associated with alluvial deposits where recharge occurs slowly with minimal gas entrainment (Segal, 2013). This research suggests insignificant mountain block fracture flow in Martis Valley. The excess air measurements reinforce the low elevation recharge dominance implications of the noble gas recharge temperatures. This suggestion, however, contradicts most Maxey-Eakin based spatial recharge estimates that are biased toward precipitation locations.

Segal (2013) also investigated groundwater flow directions based on geochemical mixing ratios. Groundwater flowing from the east picks up a mantle helium signal, likely upwelling from the Polaris fault, and then mixes with the groundwater flowing from the west. The mixing ratios observed allowed for a general estimation of groundwater flow directions (Figure 5).

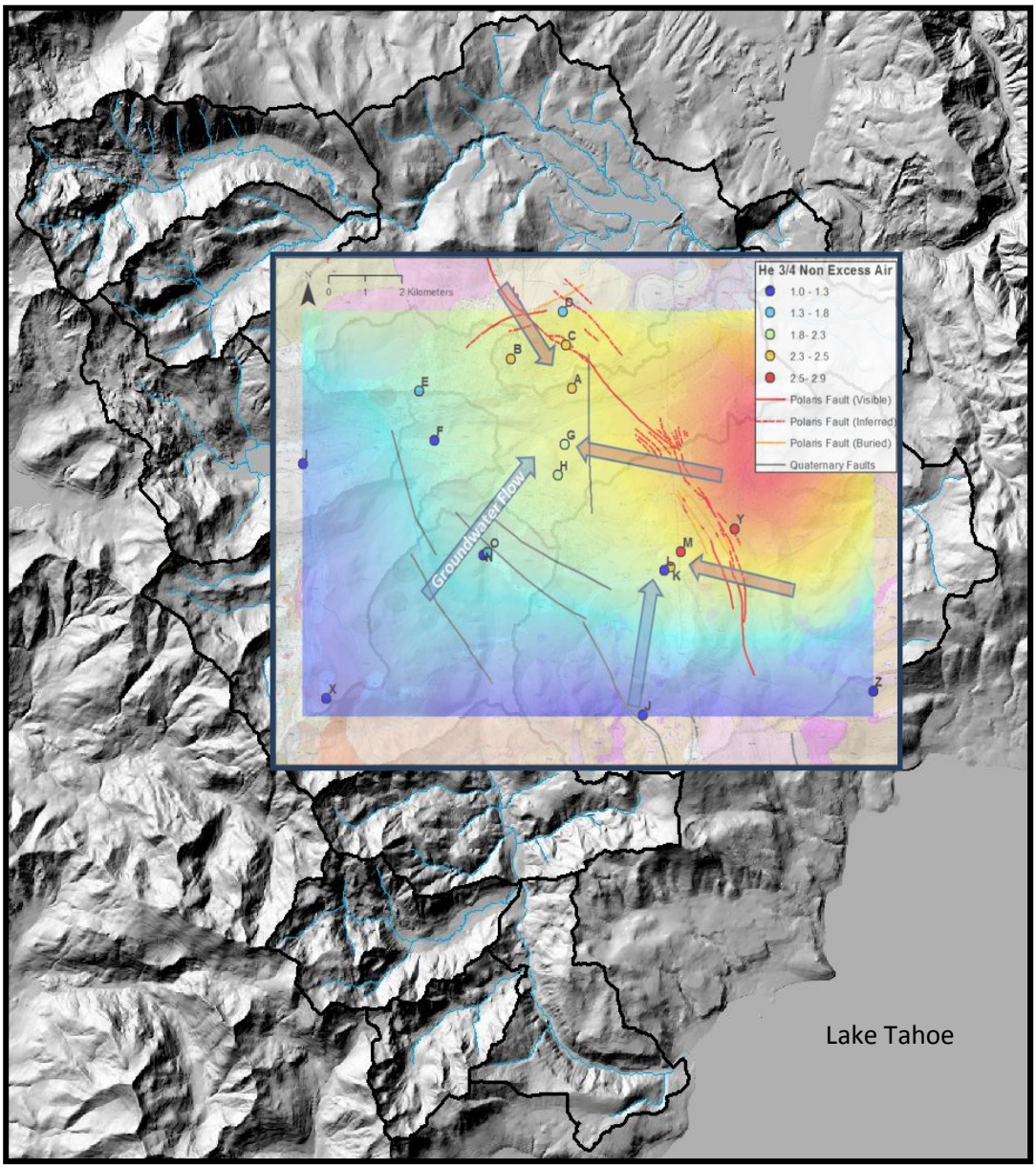

Figure 5: From Segal (2013), flow directions inferred from geochemical mixing ratios, related to fault derived mantle helium concentrations. East and west groundwater flows are estimated to converge in the central portion of the valley before discharging to the Truckee River.

Numerical Modeling

Advancement of computer codes and processing capabilities has allowed numerical modeling tools to enhance hydrologic research. Several recent studies have employed integrated modeling techniques to assess water resources (Panday and Huyakorn, 2004; Kollet and Maxwell, 2006; Ferguson and Maxwell, 2010; Sulis et al., 2011). These models incorporate feedbacks between the land surface, soil, and groundwater zones that more realistically simulate interconnected hydrologic processes compared to previous compartmentalized models. Ferguson and Maxwell (2010) used an integrated groundwater-surface water model to investigate watershed response to climate change in the southern Great Plains. One control simulation was run based on physical data from a single water year, and then three subsequent "perturbed" simulations were run to project potential scenarios onto the study area. The perturbed scenarios were used to evaluate sensitivity of the water and energy balance to changes in temperature and precipitation. Recharge and storage losses were sensitive to the perturbed scenarios. The research strongly suggested that the magnitude and seasonality of groundwater feedbacks are sensitive to changes in climate, and illustrated how integrated models can expose relationships and sensitivities of the water balance. Huntington and Niswonger (2012) used an integrated modeling approach to assess surface water and groundwater interactions under projected summertime streamflow scenarios in a snow dependent watershed adjacent to Martis Valley. The integrated modeling software, GSFLOW, was used to simulate snowmelt timing, streamflow, storage, evapotranspiration, and groundwater recharge and discharge. The simulations showed that the timing of groundwater discharge is inversely related to snowmelt runoff and groundwater recharge,

causing summertime flows to deplete even if projected precipitation and recharge increase. The results highlighted the importance of integrated modeling to study interconnected SW/GW systems.

Baseflow Analyses

Snowmelt recession and dry summers cause the baseflow component of the Martis Valley watershed to play a large role in streamflow, especially late in the water year (summer into fall). Studies have shown groundwater plays a significant role in streamflow during both high and low flow periods (Singleton 2009, Liu et al. 2004, Rademacher et al., 2005). The baseflow component of streamflow has commonly been assumed to be roughly equivalent to groundwater recharge, and several methods have been developed to investigate recharge from streamflow records (Mau and Winter, 1997; Rutledge, 1992; Rorabaugh, 1964; Mayboom, 1961). To investigate vadose zone and aquifer storage tendencies and relationships between precipitation and recharge, analyses of baseflow periods can be applied to watersheds or sub-watersheds. Kirchner (2009) showed that streamflow data, as a function of storage in a catchment, could be used to determine "catchment sensitivity". This catchment sensitivity function quantifies change in streamflow as a result of changes in catchment storage. Ajami et al (2011) applied Kirchner's recession curve-derived storage-discharge relationship as a means to quantify mountain block recharge rates. Comparing baseflow quantities to that of precipitation provides insight into recharge efficiency and aquifer storage dynamics.

Description of Study Area

Physical setting

The Martis Valley watershed occupies the northern section of the Tahoe-Truckee graben between the Sierra Nevada Range to the west and the Basin and Range Province to the east (Sylvester et al. 2007; Schweickert et al. 2011). This graben consists of the region in which both Lake Tahoe and Martis Valley basins are located. Martis Valley proper is located within the Martis Creek sub-basin and parts of adjacent sub-basins to the north. These three sub-basins make up roughly half of the watershed, which contains a total of fourteen sub-basins. The watershed is bisected by the Truckee River running out of Lake Tahoe at Tahoe City. From Lake Tahoe, the Truckee River runs north for approximately 22 kilometers where it is fed by several streams flowing out of sub-basins on the western side of the river. Once the river nears the town of Truckee, it curves to the east and continues at an east-northeast direction where it acquires dam released flows from Donner Lake, Prosser Reservoir, and Martis Creek Reservoir and natural flow from small tributaries before it leaves the basin.

The watershed covers an area of just over 500 km^2 with a maximum relief of roughly 1000 m. The lowest tiers of the valley sit around 1730 m elevation and the highest mountain peaks reach over 2700 m. Hills rise along the skirts of the valley floor and mountains make up the backdrop to the south and east of the valley. Out of the valley and into the Sierra Nevada to the west, several glaciated sub-basins comprise this western portion of the study area. To the north, volcanic dominated sub-drainages run into Prosser reservoir, which releases water into the Truckee River shortly before its exit from the study area.

The basement rock is comprised largely of andesitic and basaltic lava and volcaniclastics along with granitic plutons in the western portion. These bedrock formations are largely overlain by less consolidated volcanics and glacial, fluvial, and alluvial deposits ranging from fine clay to large boulders (Sylvester et al. 2007). At the higher elevations of the watershed, the mountain block is exposed or covered by thin layers of sediment that thicken near streambeds and eventually form the basin fill aquifer at the lower elevations, reaching thicknesses of over 200 m on the valley floor. This basin fill unit is interbedded with glacial tills, alluvial sediments, and clayey silt lenses (Sylvester et al 2007).

One major active fault runs through the study area, the Polaris fault, a right lateral strike-slip fault running southeast to north-northwest through mainly the eastern portion of Martis Valley and extending north beyond the town of Truckee and out of the study area. A recent study suggests the active Polaris fault zone may act as a potential impedance to groundwater flow (Bauer et al. 2013); however, based on water level data available for this research and numerical results from the flow model, faults were not considered substantial groundwater flow barriers.

Geologic History

The oldest rocks in the greater Tahoe-Donner region are Paleozoic sediment deposits that were metamorphosed during the intrusion of the Cretaceous Sierra Nevada batholith (Sylvester et al. 2012). These metasediments lay mostly to the west and south of the Martis Study area. The Sierra Nevada intrusive granitic rocks make up a

significant portion of the western side of the Martis watershed. Several volcanic events spanned through the Oligocene, Miocene, and Pliocene epochs, with volcanic centers reaching as far as central Nevada. These events formed what is the basement rock of the remaining portion of the Martis watershed. The interlayered volcanics can be categorized into their respective events, but for hydrologic investigations, it is more conducive to characterize the formations by their hydrogeologic properties. The volcanic rocks of the Martis basin are largely andesitic and basaltic in origin, with some rhyolitic qualities (Sylvester et al. 2012). The consolidated volcanic and granitic formations that make up the basement rock are low permeability formations. The Late Pliocene brought more local volcanic events that formed dark basalt lava flows, visible in outcroppings in the Martis basin. Quaternary glaciers caused the majority of deposition on the western half of the Martis watershed. These glacial deposits and carved valleys make up the majority of surface topography in this region, and when glacial dams that blocked outflow from Lake Tahoe finally broke, large boulders were deposited as far east as Reno (Sylvester et al. 2012). All the alluvial deposits that sit on the surface are less than one million years old and remain unlithified (Sylvester et al. 2012). It is the basin-fill alluvial layers that make up the dominating water bearing units of the Martis Valley aquifer.

Hydrographic Setting

The Martis Valley watershed is representative of many snow dominated regions of the semi-arid mountainous west, consisting of large topographic relief and relatively impermeable bedrock that causes shallow groundwater flow through alluvial soils. The basement rocks of both Miocene volcanics and Cretaceous-Jurassic plutonic rocks are

relatively low permeability and it is assumed that negligible amounts of water infiltrate into the bedrock (Rajagopal et al. 2012). The Miocene-Pliocene and Quaternary basin fill sedimentary units include lake, stream, and glacial deposits and make up the main water bearing units within the Martis basin. Low permeability clayey silt lenses extend intermittently through the basin fill formations acting as local confining layers. Lying somewhat within and largely below the basin fill sediments are weathered and fractured volcanics and granites, termed in this work "weathered bedrock", and considered to bear and transmit some water (Bauer et al. 2013).

The primary hydrologic feature of the Martis watershed is the Truckee River. Major water bodies within the hydrographic area include Donner Lake, Prosser Reservoir, and Martis Creek Reservoir. Donner Lake is naturally dammed by a glacial moraine, with additional storage created by a man-made dam. Its outlet, Donner Creek, feeds the Truckee River near central Truckee (town). Prosser Creek Reservoir collects and stores contributions from the northern portion of the watershed. The outlet of Prosser feeds directly into the Truckee River shortly before its exit from the Martis basin. Martis Creek Reservoir collects water from the Martis Creek drainages that originate in the mountainous region in the south and southeast of the study area. Because the aforementioned Polaris Fault poses a potential seismic hazard to the Martis Creek Reservoir dam, the reservoir is not utilized to its full potential, and fluctuates very little acting mainly as a flood control feature (Hunter et al. 2011).

Stream gages in the watershed are located in the Truckee River near the town of Truckee and at the outlet of the basin, and also along the outflows of Donner Lake, Prosser Creek Reservoir, Martis Creek Reservoir, and in Squaw Creek in Squaw Valley.

Two SNOTEL sites lie within the study area: Truckee #2, located in the center of the basin at 1984 m elevation near the Truckee Airport, and Squaw Valley G.c., located in the Squaw Valley sub-basin at 2447 m elevation (Figure 6).

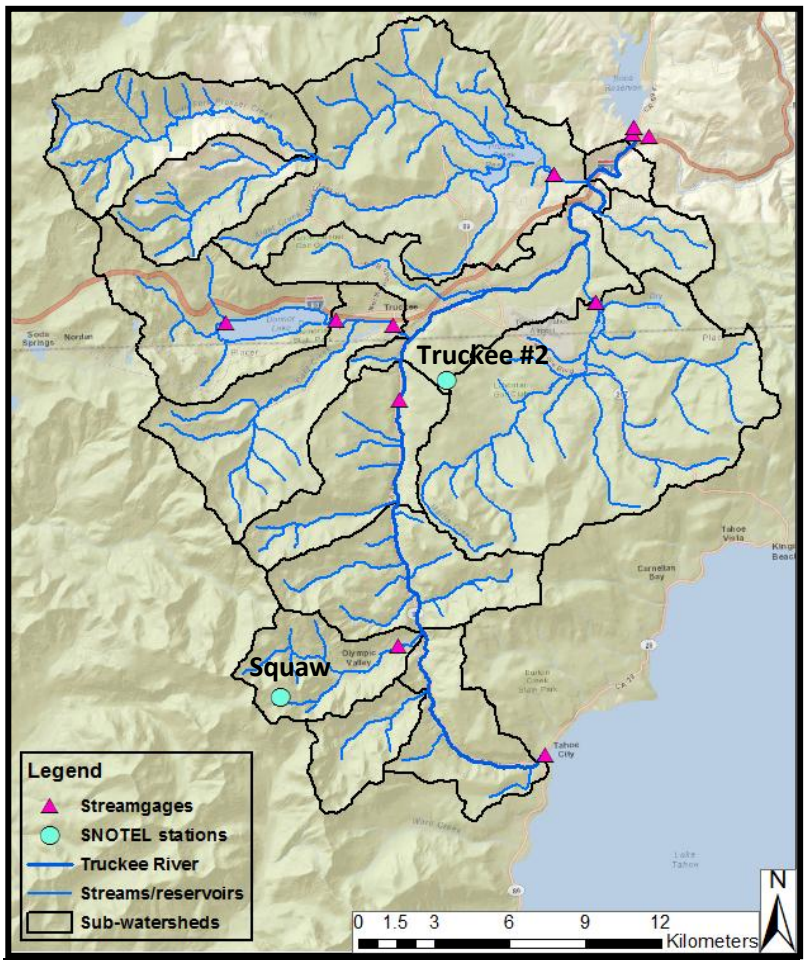

Figure 6: Martis watershed with delineated sub-basins, stream networks, streamgages, and SNOTEL site locations and names.

Climate and Vegetation

The climate of Martis Valley is congruent with that of the greater Lake Tahoe-Truckee region: warm, dry summers that produce sporadic thunderstorms, and cold, wet winters that bring the majority of precipitation to the watershed as snow. Elevation and

rain shadow effects significantly influence the spatial variability of temperature and precipitation in the basin. The upper elevations of the southern and western portions of the basin receive the most precipitation, typically from Pacific Ocean marine air masses. These higher elevations (above 2050 m) receive a mean annual snow water equivalent of over 115 cm, while approximately 75 cm falls annually below this level. Annual peak streamflow typically occurs during spring snowmelt, although the hydrograph also responds to periodic mid-winter rain on snow events. The region experiences high climate variability, marked by wet and dry periods. Figures 7a and 7b show the mean monthly precipitation distribution recorded at the Truckee #2 and Squaw SNOTEL sites, respectively. Figure 7c shows mean monthly streamflow at the USGS Truckee River gage near downtown Truckee. Based on data from the Truckee #2 SNOTEL Station, average temperatures range from highs of 28ºC in July to lows of -9ºC in December and January. Droughts are common in this region of the Sierra Nevada, and tend to last longer than the short lived, but more extreme wet periods. Vegetation ranges from dense coniferous forests in the highest and wettest areas of the watershed to open forests mixed with grasses, sagebrush, and rabbit brush in the drier, lower elevations.

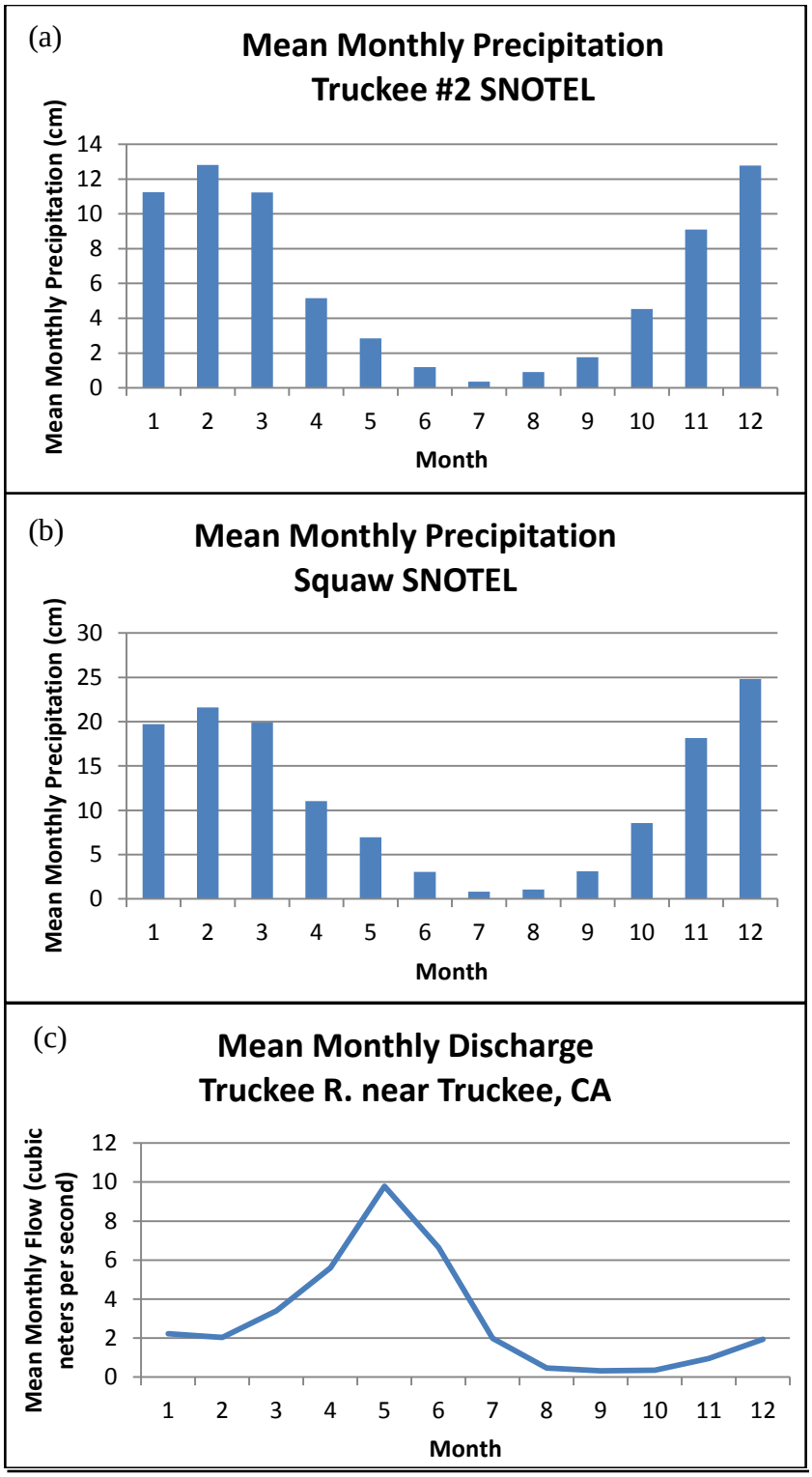

Figure 7: Mean monthly precipitation in centimeters of water recorded at (a) Truckee #2 and (b) Squaw SNOTEL sites from 1980-2013. (c) Mean monthly streamflow measured in the Truckee River near downtown Truckee by the USGS stream gage from 1980-1982 and 1992-2010.

Water use

Because of the semi-arid setting, a highly variable climate, and increased water demands from the greater Truckee-Donner and Reno areas, water resources and reservoirs are highly managed. The Truckee-Donner Public Utility District (TDPUD) controls thirteen active production wells that provide the greater Truckee area with potable water, plus three wells to serve non-potable demands; while the Truckee River flows through this region without diversion (Bauer et al. 2013). The TDPUD reported in 2010 that the potable water demand of the Truckee area was 6.25 million cubic meters per year (5,073 acre-feet per year). Northstar Community Services District (NCSD) and Placer County Water Agency (PCWA) control two production wells each within Martis Valley, meant to serve the Northstar recreation operations and the Lahontan Golf Club and community, respectively. The total estimated average water demand for the Martis Valley groundwater basin is 11.5 million cubic meters per year (9,341ac-ft/yr) (Bauer et al. 2013). Several private wells are distributed through communities across the basin and in outlying home tracts. The city of Reno and its outlying communities demand much more water for municipal, domestic, industrial, and recreational uses. This water supply depends heavily upon the Truckee River and Martis Valley watershed contributions, and reservoir management. Eighty-five percent of Reno's water supply comes directly from the Truckee River, while the Truckee-Donner communities depend completely on groundwater in Martis Valley (Bauer et al. 2013).

Streamflow from Lake Tahoe, Donner Lake, Martis Creek, Prosser Creek, and the Little Truckee is controlled by dam operations. The timing and amount of flow released is governed by several court decrees, agreements, and regulations. The streamflow rates,

designated in the Truckee River Agreement of 1935, and termed ‘Floriston Rates’, are measured at the Farad, CA USGS gaging station, just before the Truckee River enters Nevada. According to the Truckee River Operations manuscript, mean flow rates at the Farad USGS gage must be kept to an average of 500 cubic feet per second (cfs) in the summer and 400 cfs in the winter, with some flexibility based on the level of Lake Tahoe (Summary Truckee River Operations, 2002). These rates are designated to support irrigation and municipal demands downstream, as well as provide hydroelectric power. According to the Truckee Meadows Water Authority (TMWA) 2010-2030 Water Resources Plan, there is approximately 175 million cubic meters per year (142,000 ac-ft/yr) of decreed, storage, and irrigation rights from which annual water supplies can be generated. These resources come from reservoir and groundwater storage, as well as surface water supplies, all within the Truckee River Basin.

Methods

The approach taken to investigate and simulate groundwater recharge in the Martis watershed is discussed in the following sections. Descriptions and methodologies of the baseflow analysis, stable isotope investigations, framework grid development, and PRMS, MODFLOW, and GSFLOW models, are provided in the following sections.

Baseflow analysis

Analysis of hydrograph baseflow recession curves can be used to identify the parameters of a conceptual catchment storage model (Lamb and Beven, 1997). A recession curve refers to the falling limb of the hydrograph along which no precipitation occurs. Because baseflow is dominated by groundwater, baseflow recessions and baseflow periods of the hydrograph can be related to groundwater recharge. Using data from streamflow gages and National Resource Conservation Service (NRCS) SNOTEL sites (Figure 6), baseflow periods for the Martis Creek sub-watershed were analyzed to form initial relationships between precipitation, streamflow, and baseflow.

Spatial precipitation data were available from the Parameter-elevation Regressions on Independent Slopes Model (PRISM) database, which uses point data from climate stations, such as SNOTEL sites and cooperating National Weather Service (NWS-Coop) stations. PRISM uses physiographic factors to create a precipitation grid over the area of interest based on the nearest data stations. According to the manuscript describing the development of the PRISM database, climate–elevation regression is developed from pairs of elevation and climate measurements provided by station data (Daly et al., 2008). Annual precipitation amounts in the Martis Creek sub-watershed

were compared to annual streamflow and baseflow of Martis Creek. Figure 8 shows the mean annual precipitation over the entire watershed, based on the PRISM technology.

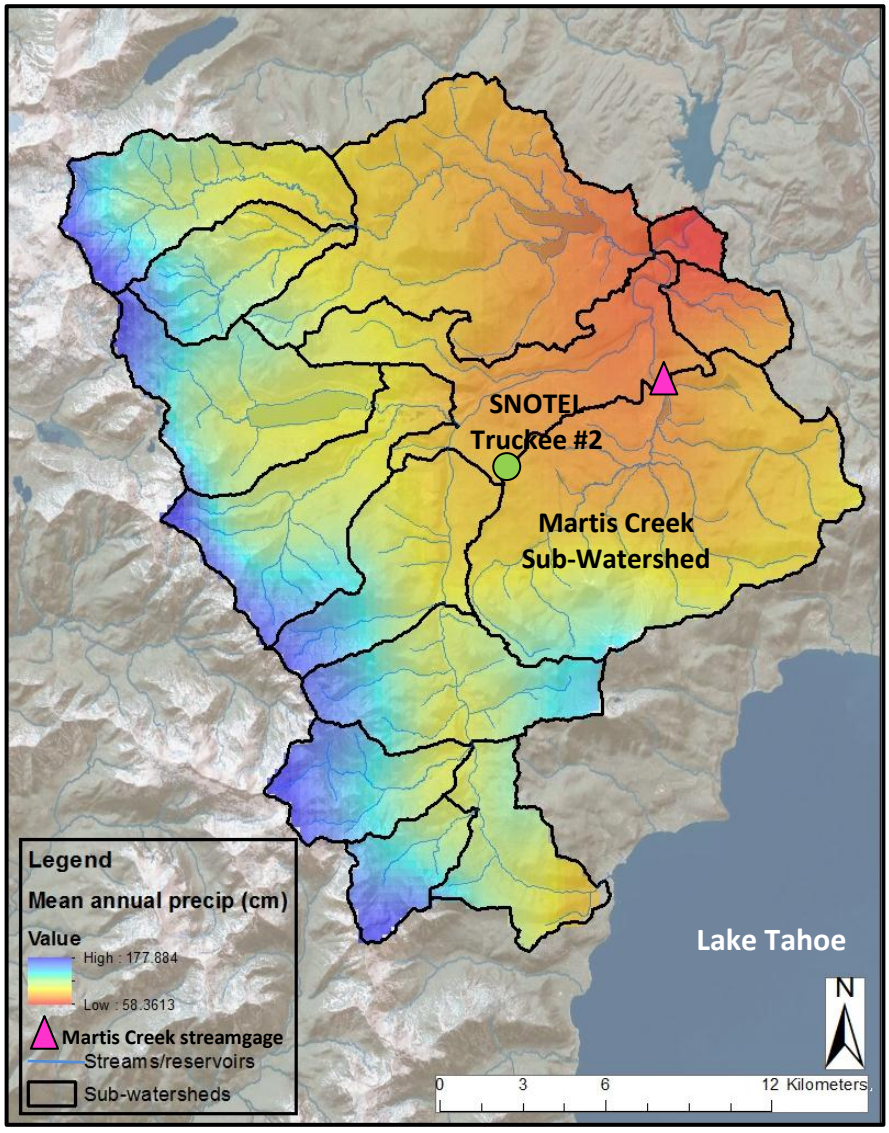

Figure 8: PRISM distributed mean annual precipitation. Note that the large majority falls along the upper elevation mountainous corridor on the western edge of the watershed. Also shown are streamflow gage and precipitation site locations used for the Martis Creek baseflow analysis.

Daily average discharge rates were obtained for Martis Creek in cubic feet per second (cfs) from October 1, 1980 to September 30, 2011. It is important to note that the

streamgage in Martis Creek sits just below the dam that creates Martis Creek Reservoir, and therefore the streamflow values were naturalized in order to simulate the natural streamflow without the dam. The naturalized data through September 30, 2000 comes from a dataset known as TCDATFIL, developed by several stakeholders in the Truckee Basin. These data were designed for the Truckee River Operating Agreement (TROA). The naturalization calculation is based on reservoir stage-volume relationships, or reservoir water budget estimation. Blodgett et al. (1984) provides more detailed information on streamflow naturalization. The streamflow values beyond Sep. 30, 2000, naturalized by the Federal Water Master's office, were intermittent. Thus, only the continuous data period from October 1, 1980 through September 30, 2000 was used for baseflow analyses.

From the Martis Creek daily discharge data, a three month baseflow period for each year was selected to compute an average daily baseflow. Because of variation in the timing and length of snowmelt, the baseflow period shifted between June and October. For example, June 30 to September 30 was chosen as the main three month baseflow period for 1981, but the following year, July 15 to October 15 was chosen (Figure 9). This method was used in order to gather averages from the lowest flows of the year, which are most likely to be completely groundwater derived. These three month averages were then extended for the entire year to estimate annual baseflow volumes. Annual baseflow volumes were then compared to annual streamflow and precipitation volumes. The annual baseflow volumes considered are conservative as they do not account for any increase in baseflow contribution throughout the year. This was acceptable for initial estimations because the goal of developing baseline relationships

between baseflow, streamflow, and precipitation volumes was still attainable from the analysis. Annual fractions of baseflow (Qbase) and streamflow (Q) to precipitation (PPT) were computed to quantify the Qbase – Q – PPT relationships over the entire 20 year period.

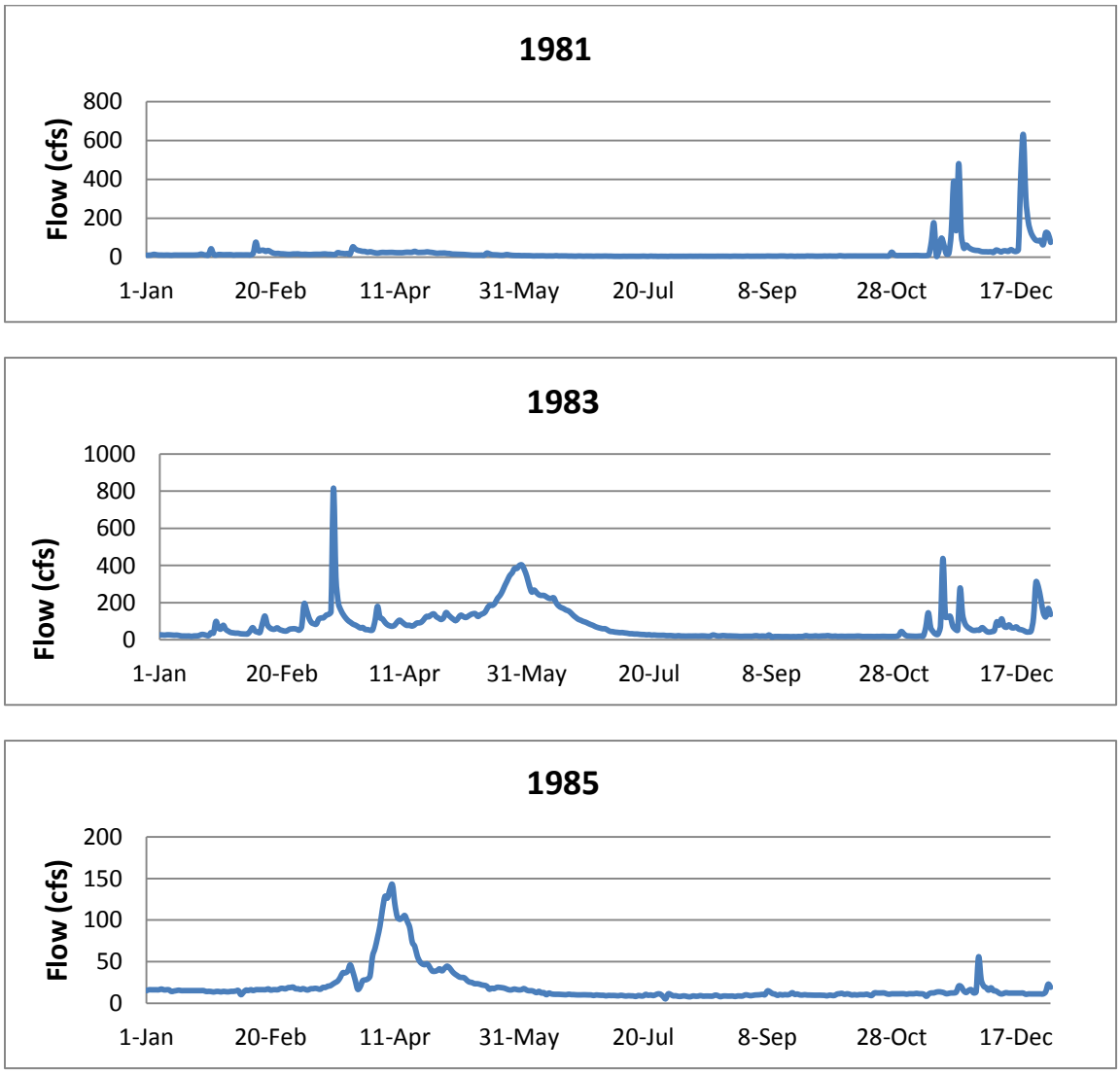

Figure 9: Three annual Martis Creek hydrographs, illustrating variations in baseflow period. 1981 shows baseflows spanning from May through October, while 1983 doesn't exhibit baseflow levels until late July. 1985 falls in between showing baseflows from June through September.

Stable Isotope Analysis

Stable isotopic data from Lawrence Livermore National Laboratory (LLNL) included deuterium ($\delta^{2}H$) and oxygen-18 ($\delta^{18}O$) measurements of groundwater, surface water, and snowmelt from Martis Valley throughout 2012. Stable isotopes can be used to identify the source and timing of recharge, and can provide valuable information on evaporation rates and flow processes in the unsaturated and saturated zones (Healy, 2010). The measured isotopic values were recorded as parts per thousand or permil Vienna Standard Mean Ocean Water (‰ VSMOW). LLNL had not performed any preliminary analysis or interpretations of the stable isotope data prior to sharing the data. Although one year of data does not allow for an incredibly robust analysis, basic comparisons between sample types were still able to be observed.

Once a snowfall event has taken place, the isotopic signature of this event will evolve within the snowpack over time because of isotopic fractionation, or changes in isotopic abundance ratios. Phase changes, evaporation, condensation, freezing, sublimation, melting, and some chemical reactions are all associated with isotopic fractionation (Leibundgut et al., 2009). Isotopic fractionation processes, plus a below average snowpack in 2012, make the isotopic storm signatures in streamflow samples more difficult to interpret; however, they still held a unique enough signal to reveal basic processes.

Preliminary analyses of the isotopic data included observing the surface, groundwater, and snow samples over time to detect seasonal fluctuations and form relationships between the sample types. Groundwater was only sampled in the summer, however, so a time series was not available. Stream samples from two separate reaches

of Martis Creek were taken throughout 2012, so an annual time series representing streamflow was observed. Snow samples had been taken over the course of the winter and spring months at three locations above Martis Valley in order to obtain isotopic signatures of the snowmelt, and variations thereof were observed.

The isotopic data was plotted along a global meteoric water line (GMWL). Observing the relative isotopic enrichments along the GMWL provided information on seasonal fluctuations and fractionation processes. Snowmelt isotopic data were observed with model simulated snowmelt timing and magnitude to determine the effects of snowmelt on isotopic signatures of the snowpack, which are reflected in groundwater and stream samples. Isotopic streamflow data from two forks of Martis Creek were observed with model simulated Martis Creek hydrograph after the convergence of the forks to determine isotopic fluctuation related to discharge timing and magnitude.

Numerical Modeling

The Groundwater Surface-Water Flow (GSFLOW) model (Markstrom et al., 2008) used for this research couples the Precipitation Runoff Modeling System (PRMS) (Leavesly et al., 1983) with the Modular Groundwater Flow (MODFLOW) model (Harbaugh, 2005), and creates an integrated SW/GW simulation. Driven by temperature and precipitation data, GSFLOW was used to simulate all surface and groundwater hydrologic processes within the Martis watershed. GSFLOW simultaneously accounts for climatic conditions, runoff across land surface, variably saturated subsurface flow and storage, and connections among terrestrial systems, streams, lakes, wetlands, and

groundwater (Huntington and Niswonger, 2012). Markstrom et al. (2008) and Niswonger et al. (2011) provide a complete description of GSFLOW and its theory.

PRMS is a physical process based, deterministic modeling system developed to evaluate watershed response to various climate and land use combinations (Leavesley et al., 1983). PRMS simulates snowpack in terms of water storage and as a dynamic heat reservoir (Jeton and Maurer, 2011). Surface runoff can flow to the four neighboring surface grid cells, infiltrate, or flow to a stream. Preferential, capillary, and gravity reservoirs represent the different components of soil storage properties, and control whether water will percolate deeper (MODFLOW), flow horizontally to a receiving grid cell or stream, or evapotranspire to the atmosphere (Huntington and Niswonger, 2012). Groundwater will contribute to soil zone storage if the water table is above the base of the soil zone, and will discharge to the surface if groundwater heads are above land surface. Potential evapotranspiration (PET) is first derived from vegetation canopy interception-storage, followed by sublimation and impervious surface evaporation. Evapotranspiration (ET) is simulated as a function of PET. McDonald and Harbaugh (1988), Markstrom et al., (2008) and Huntington and Niswonger (2012) provide further details on the PET simulations and theory. Spatial heterogeneity is accounted for by a "distributed parameter" representation of spatially varying hydrologic characteristics. Model parameterization is based on digital elevation maps and datasets describing soil type, land cover, and stream networks. The varying parameters are numerically represented as a collection of hydrologic response units (HRUs). Water and energy balances are computed daily for each HRU. Martis Valley HRUs are grid based and

assumed to contain homogenous hydrologic response characteristics within each grid cell.

Flow below the base of the soil zone was simulated by MODFLOW. The version of MODFLOW used for this application of GSFLOW was MODFLOW-NWT, a Newton formulation of MODFLOW-2005 that accurately simulates drying and wetting of groundwater cells (Niswonger et al., 2011). MODFLOW is a finite difference, three-dimensional groundwater flow model that simulates steady and transient flow in irregularly shaped flow systems in which aquifers can be specified as confined, unconfined, or a combination of both (McDonald and Harbaugh, 1988; Harbaugh and McDonald, 1996; Harbaugh and others, 2000). Hydraulic conductivities for any layer may be heterogeneous and anisotropic and storage coefficients may be heterogeneous. Specified head and flux boundaries can be simulated as well as head dependent flux over the model boundary that allows water supply to a boundary cell at a rate proportional to the current head difference between the source and boundary cell (Harbaugh 2005). The groundwater flow equation is solved using a finite difference approximation. The flow model is subdivided into cells that are assigned medium properties, much like the HRUs of PRMS. The groundwater flow equation is solved iteratively for each active model cell according to assigned hydraulic parameters and applied sources and sinks.

The Martis Valley MODFLOW model is forced by mean annual infiltration (PRMS), distributed by the Stream Flow Routing (SFR2) package (Niswonger and Prudic, 2005) and Unsaturated Zone Flow (UZF1) package (Niswonger et al., 2006). Flow-rate and cumulative-volume balances from each type of inflow and outflow are computed at each time step (Harbaugh 2005). Boundary cells are designated as specified

head, constant head, variable head, or no-flow in order to define the boundary conditions. Harbaugh (2005), Niswonger et al. (2011), and Huntington and Niswonger (2012) provide more information on MODFLOW and its solver packages.

The work for this thesis focused on the development of a hydrogeologic framework model (HFM) upon which the MODFLOW simulation operated. A production well pumping database was also constructed for model input. HFM grid development began with well log evaluations and database construction. Over 300 well logs were obtained from the California Department of Water Resources (DWR), Truckee Donner Public Utility District (TDPUD), Placer County Water Agency (PCWA), and the Northstar Community Service District (NCSD). A master well log database was built containing all available information from the well logs. For well logs missing spatial information, the centroid of the parcel (if provided) was designated for the well location. If the parcel number was also unavailable, a driller's sketch of the location could sometimes be deciphered. Apart from location, other relevant information for model development included depth to bedrock, depth to water, drawdown and specific yield, and subsurface geologic data. To better understand the depth, thicknesses, and extent of the geologic formations comprising the basin, a lithologic numbering system was created to categorize the subsurface data. Previously, Brown and Caldwell with Balance Hydrologics, Inc. developed a lithologic classification system based off Martis Valley well logs and geologic formations (Bauer et al., 2013). Their classification scheme contained six units: 1. glacial outwash 2. alluvium 3. unconsolidated volcanics/sediments 4. interbedded clays/sediments/gravels 5. consolidated andesite, and 6. granites. Along with Brown and Caldwell's work, geologic, hydrogeologic, and geophysical

investigations (Sylvester et al., 2007; Thodal, 1997; Plume et al., 2009; Hunter et al., 2011; Bedrosian et al., 2012; Niblach, 1988) were interpreted to develop a modified classification scheme for the Martis HFM.

To maintain a balance between hydrogeologic grid discretization and computing efficiency, adjacent geologic formations were classified as one hydrogeologic unit if their hydrologic properties were similar. For example, layers 3 and 4 of the Brown and Caldwell units were aggregated into a single layer for the HFM. For hydrologic modeling purposes, geologic details are not as crucial as hydrologic properties. Thus, horizontal and vertical hydraulic conductivites (K_h and K_v, respectively) were applied to hydrogeologic units to account for certain geologic influences. For example, the main hydrologic difference between the top two geologic formations in Martis is caused by higher clay content in the underlying formation. These clay lenses are extensive at times and can be relatively impermeable to groundwater flow (Sylvester et al., 2007). The clay formations were not specifically mapped in the HFM, but were considered when assigning hydraulic conductivity values to the layer. The final lithologic numbering system for the Martis HFM consisted of four units: 1) fine sediments, alluvial deposits, gravel, cobbles, and some boulders, with low clay/silt content, and high water bearing capabilities, 40 m maximum thickness; 2) fine to coarse sediments; fluvial, glaciofluvial, and lacustrine deposits, with pebbles to boulders, intermittent clay/silt lenses, some fractured volcanics, and slightly lower water bearing capabilities compared to layer 1, 200 m maximum thickness; 3) “weathered bedrock” unit with fractured andesites and granites, some coarse grained sediments, and low water bearing capabilities, 60 m thick;

4) bedrock, very low permeability, considered the confining unit, made up largely of competent granite, granodiorite, and andesite, 130 m thick.

The compiled lithologic data was input into the geologic modeling software, Leapfrog (ARANZ Geo, 2010), for preliminary subsurface extrapolation and visualization. The capabilities of Leapfrog were limited to data rich zones, located largely in the developed areas of the basin (Figure 10) and were found inadequate for extending the HFM into the data-scarce mountain block regions.

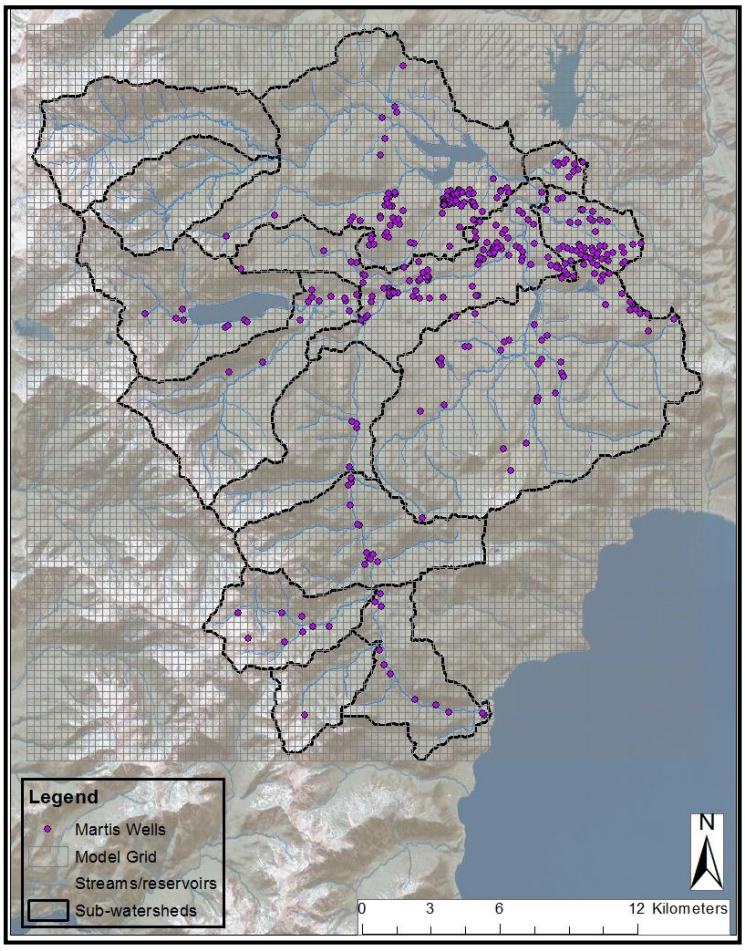

Figure 10: Well locations throughout the Martis watershed, largely consolidated near community developments. Note: not all well logs contained significant subsurface information.

The Martis watershed is similar to the greater Lake Tahoe area in that drainages in the mountain block are overlain by thin stream deposits that gradually thicken with decreasing elevation (Plume et al., 2009). Thus, where well log data was sparse or unavailable, manual adjustments were made in GIS. Alluvial thicknesses for the top two layers were designated along streambeds, starting at 5 m thick in the mountain block and gradually increasing to the data-based thicknesses of the valley (Figure 11). This maintained layer continuity and promoted more accurate simulations of surface and subsurface flow. In this way, grid block representations of the subsurface geology were a combined result of data-driven hydrostratigraphy and conceptual understanding of the surface and groundwater systems.

Model cells were set to a square 300 m spatial resolution over the 500 km^2 model domain. The grid resolution sufficiently captured elevation distribution within the model domain. Because of the steep, mountainous topography along the edges of the watershed, no-flow boundary conditions were assigned to coincide with the watershed divides. Development of the model grid depended on conditioning the digital elevation model to the model grid scale to ensure proper location of streams and wetlands (Huntington et al., 2013). Because the digital elevation model for Martis is 10 m resolution and the model grid is 300 m resolution, the elevation grid was "upscaled" to ensure that topographic highs and lows were in the correct location on the model grid. To maintain surface and subsurface flow continuity, flow accumulation and flow routing procedures were applied in GIS. These techniques created gridded datasets that could be analyzed (and adjusted if needed) to certify that surface runoff maintained a down-slope direction and subsurface flow maintained continuity throughout each layer.

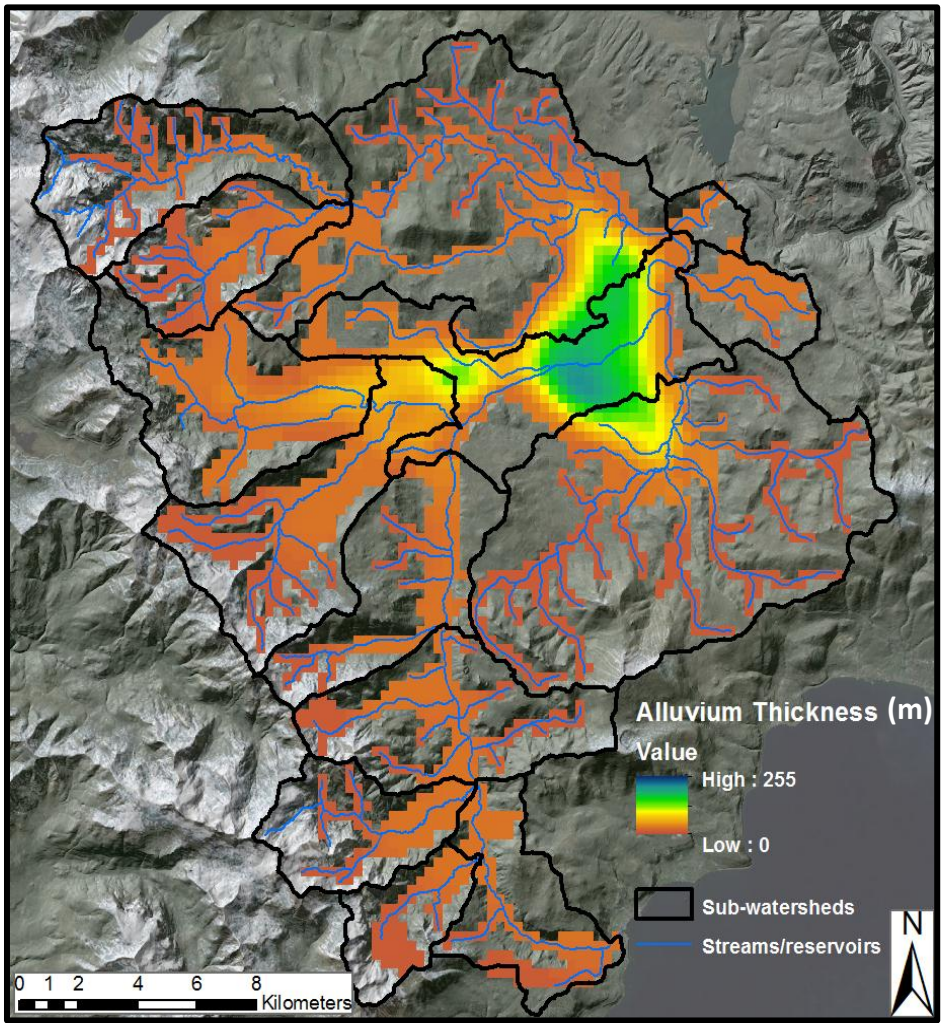

Figure 11: HFM grid total alluvium thickness, starting with a minimum of 5 m in the high elevation drainages with gradual thickening into sub-basins and the principal basin fill aquifer.

The final HFM acts as the basis through which the MODFLOW simulation operates and performs its flow calculations. This framework contains parameters for each individual grid cell, including hydrologic and physical properties. The principal goal around HFM development was parsimony, so as to create a model that balanced detailed hydrogeologic grid properties with efficient computer processing.

Recharge Methods

The GSFLOW simulation calculates recharge and discharge within each 300 x 300 m cell for each daily time step. This is calculated in the Unsaturated-Zone Flow (UZF1) Package that solves a one-dimensional form of Richards' equation (Markstrom et al., 2008). The model outputs a file containing basin wide recharge for each daily time step. Total annual recharge was compared to total annual precipitation. Annual averages were computed, and annual recharge efficiencies were determined based on recharge – precipitation ratios. Basin wide annual average recharge estimations were calculated from the daily values. In order to observe spatiotemporal fluctuations, mean monthly recharge grids were extracted from the model simulation. Annual averages were calculated from the monthly means, and temporal variations were investigated at basin and sub-basin scales. Annual and seasonal fluctuations were observed using GIS. An average annual recharge map was created from annual means over the entire simulation period to show spatial recharge trends throughout the Martis watershed. The watershed was subdivided into three elevation-based sections and recharge rates were computed for each elevation zone. Sub-basin contributions were computed from the final recharge map, and recharge rates were normalized by sub-basin areas. Results were compared to previous water balance recharge estimations and geochemical implications of recharge distribution.

Results

Baseflow Analysis Results

Results regarding the baseflow, streamflow, and precipitation relationships in the Martis Creek sub-watershed are presented in the table and graphs below. Percentages are based on the PRISM precipitation. The numbers reveal, on average, that streamflow makes up roughly half of mean annual precipitation, and baseflow is roughly one-sixth of annual precipitation (Table 2). The PPT-Q-Qbase relationship is easier to visualize graphically (Figure 12).

Year	Total Streamflow % of annual precip	Baseflow % of anunal precip
1981	29.37	5.37
1982	61.81	15.06
1983	80.73	19.50
1984	81.21	35.25
1985	51.72	24.89
1986	85.78	23.51
1987	34.05	17.15
1988	25.18	15.26
1989	34.16	10.98
1990	27.70	11.50
1991	19.19	10.93
1992	15.58	7.72
1993	61.30	10.94
1994	16.96	7.14
1995	62.79	19.51
1996	42.88	10.09
1997	87.64	21.23
1998	52.32	16.67
1999	72.26	24.07
2000	48.20	18.74
Mean	**49.54**	**16.28**

Table 2: Mean annual baseflow and streamflow percentages of annual precipitation for Martis Creek from 1981-2000.

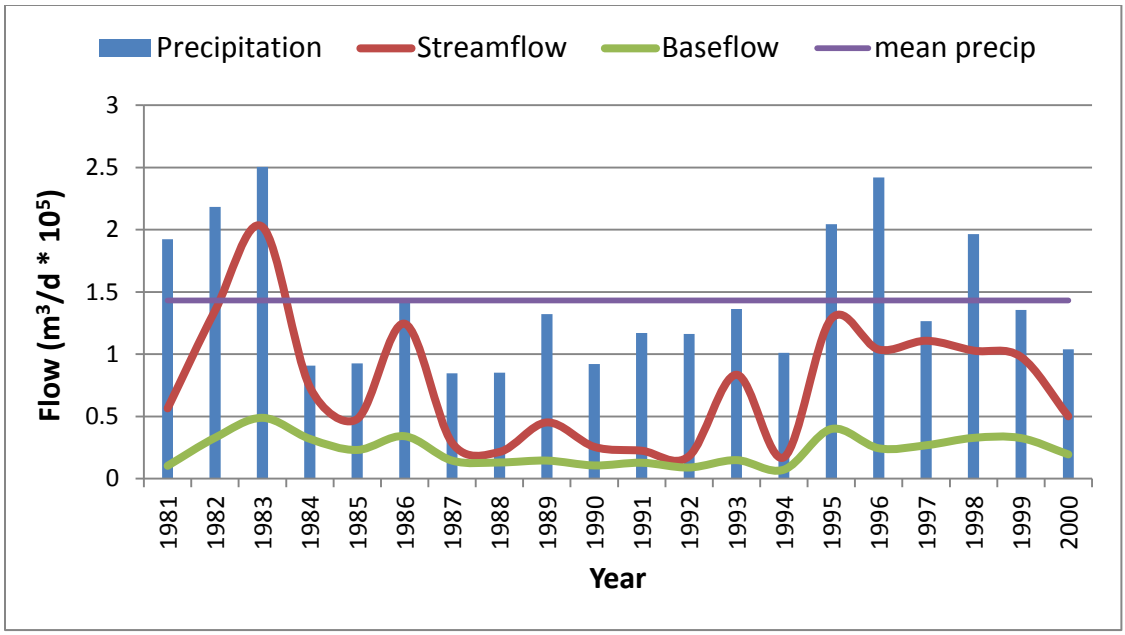

Figure 12: Time series from 1980-2000 of mean annual precipitation, streamflow, and baseflow volumes in the Martis Creek sub-watershed, illustrating annual fluctuations and responses to precipitation trends.

As seen in Figure 12, 1981-1983 were high precipitation years. Streamflow and baseflow both respond with increasing flows as expected. The drop off in precipitation that follows is also reflected in the streamflow and baseflow. However, after two relatively dry years (1987 and 1988), baseflow is less responsive to the following precipitation and streamflow increase, and remains relatively unresponsive until heavier precipitation falls in 1995. Precipitation in 1984-1985 is as low as that of 1987-1988, but streamflow and baseflow in 1984-1985 is much higher than in 1987-1988. Although large fluctuations in precipitation occur from 1996 to 1999, the streamflow and baseflow components remain relatively steady. Baseflow generally fluctuates with streamflow, but appears to be less reflective of precipitation after consecutive low precipitation years. Both streamflow and baseflow components seem to be less responsive to precipitation

fluctuations after several years of below average precipitation. It can be observed that during 1991 and 1992, baseflow made up roughly half of streamflow. This seems to be the result of multiple below average precipitation years. Overall, it is clear that annual changes and trends in precipitation drive annual changes in groundwater flux, and consecutive high or low precipitation years have residual effect on streamflow and baseflow response in years following.

Stable Isotope Results

Stable Isotope data was investigated to highlight possible recharge sources and produce reasonable relationships between precipitation, runoff, groundwater, and streamflow. Even with the sparse data, it is clear that snowmelt has a direct effect on streamflow and that groundwater is made up largely of winter precipitation (Figure 13).

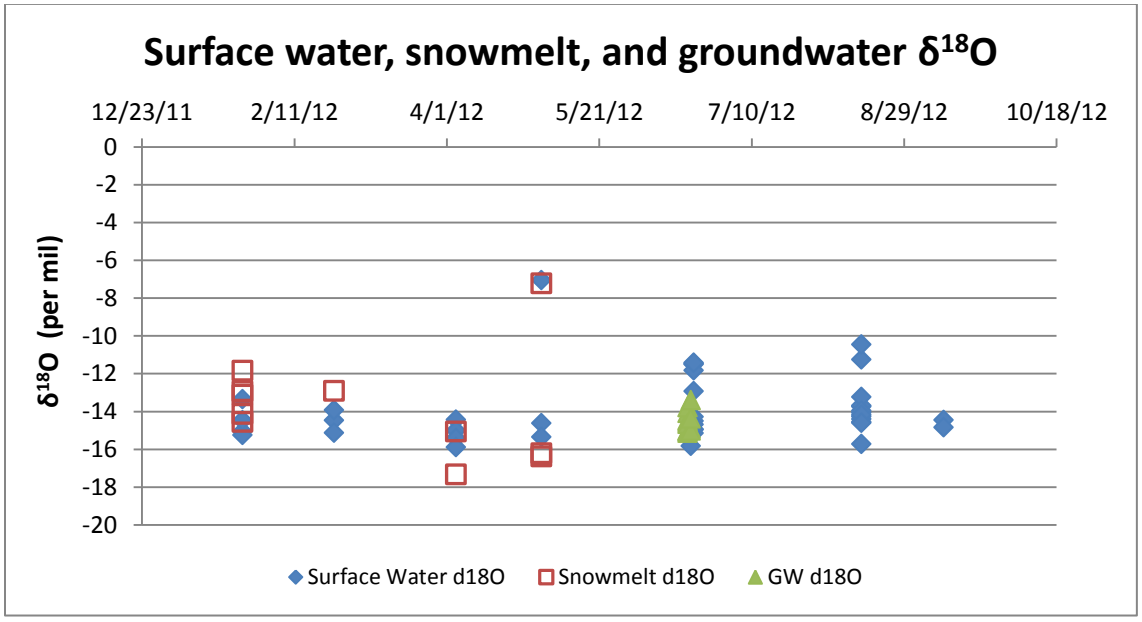

Figure 13: $\delta^{18}O$ signatures of surface water, snowmelt, and groundwater over time ($\delta^{2}H$ data showed similar relationships).

It can be observed in Figure 13 that during peak runoff in spring months, the surface water expresses the most depleted (most negative) values, reflecting snowmelt measurements. Snowmelt samples become more enriched (less negative) thereafter. A progression to more enriched values in streamflow then occurs over the following months. The enriched surface water values in early May and mid-August coincide with late snowmelt and rainfall events, respectively.

Deuterium-oxygen measurements plotted along a global meteoric water line (GMWL) display the isotopic signal change and deviation from the global standard, from initial precipitation to recharge to discharge over a year (Figure 14). Winter snow samples compared to spring snow samples indicate annual climate tendencies, and can help discern streamflow composition. Isotopic signatures of snow compared to those of groundwater show that winter precipitation is the dominating contributor to groundwater recharge. Summer rainstorm events would leave a more enriched isotopic signature that is not seen in the groundwater samples. Surface water samples compared to snow samples over the year confirm conceptualizations of the influence of winter precipitation on streamflow during spring runoff. These processes indicated by the isotopic variations help verify conceptualizations and can be compared to modeled results in order to cross-check methods and gain further detail on hydrologic relationships of the system.

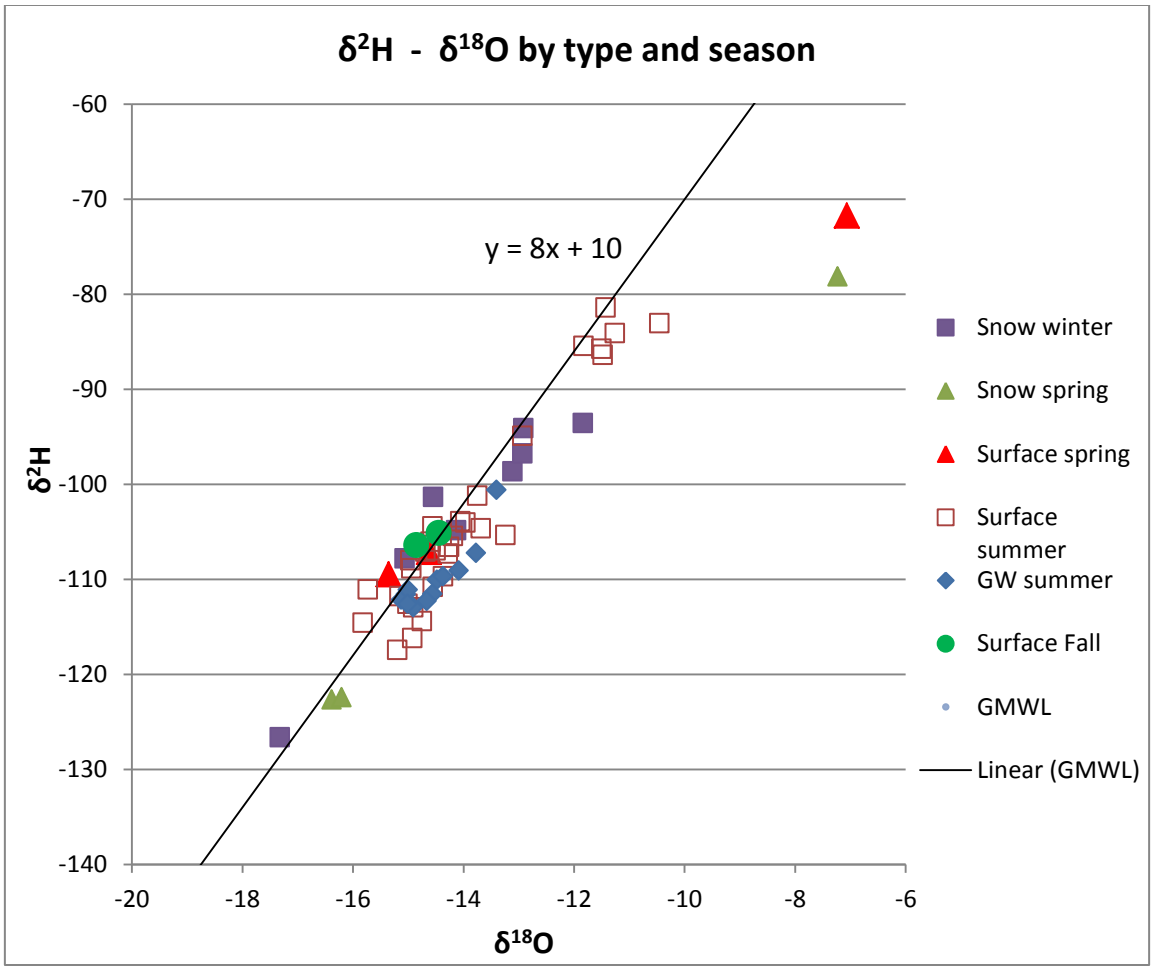

Figure 14: δ^2H-$\delta^{18}O$ along the GMWL (dark solid line) displays snowpack isotopic evolution and suggests a stronger sublimation effect over evaporation.

The δ^2H-$\delta^{18}O$ plot compares the isotopic samples by type and season (i.e. snow, spring). Snow samples fall to the left, along the middle, and slightly to the right of the GMWL. The groundwater samples fall largely to the right, indicating that fractionation is occurring at some point between deposition and groundwater recharge. One would naturally assume evaporation plays a part in this fractionation process, but the groundwater samples do not plot along an evaporation-like slope, which would typically be higher on the GMWL and trending to the right. Rather, the GW samples, all taken

during the summer, plot directly below the majority of snow samples. In an isotopic analysis of groundwater in south central Nevada, Rose and Davisson (2002) found similar results. They concluded that kinetic isotope fractionation effects occurred as the snowpack aged, resulting from vapor loss prior to melting. This can be more easily described as sublimation. This same phenomenon is likely happening in Martis Valley as snow metamorphism takes place while the weather is still too cool for significant melting and subsequent evaporation. These findings offer conceptual insight to tendencies of the system and discrete seasonal processes that can effect downstream measurements.

Model Results

Calibration

The calibration procedure requires PRMS and MODFLOW input parameters to be adjusted until model simulations equilibrate with measured values (i.e. groundwater heads and streamflow). Model calibration begins by calibrating the transient PRMS and steady-state MODFLOW models independently, followed by the GSFLOW integrated mode calibration. Model calibration is a crucial step in the modeling procedure. The Martis Valley model development was a large collaborative effort, and calibration was performed by fellow researchers at DRI. The figures in this section were obtained from their work. The calibration procedure/results will be discussed herein, although details of its interworkings lay outside the scope of this thesis project.

The calibration process is an iterative cycle of parameter adjustments followed by comparisons between simulated and measured values. PRMS calibration occurred as a stepwise process, considering annual streamflow, solar radiation, potential ET, and rising

and recession hydrograph limbs. The Martis MODFLOW model utilizes the unsaturated zone package (UZF1), streamflow routing package (SFR2), and the lake package (LAK) and was driven in steady-state by the average annual PRISM precipitation data from 1980 to 2012. Calibration targets for the MODFLOW model were wetland and riparian zones (48 cells), head measurements (14 monitoring wells/19 additional static water levels), streamflow, and reservoir/lake stage.

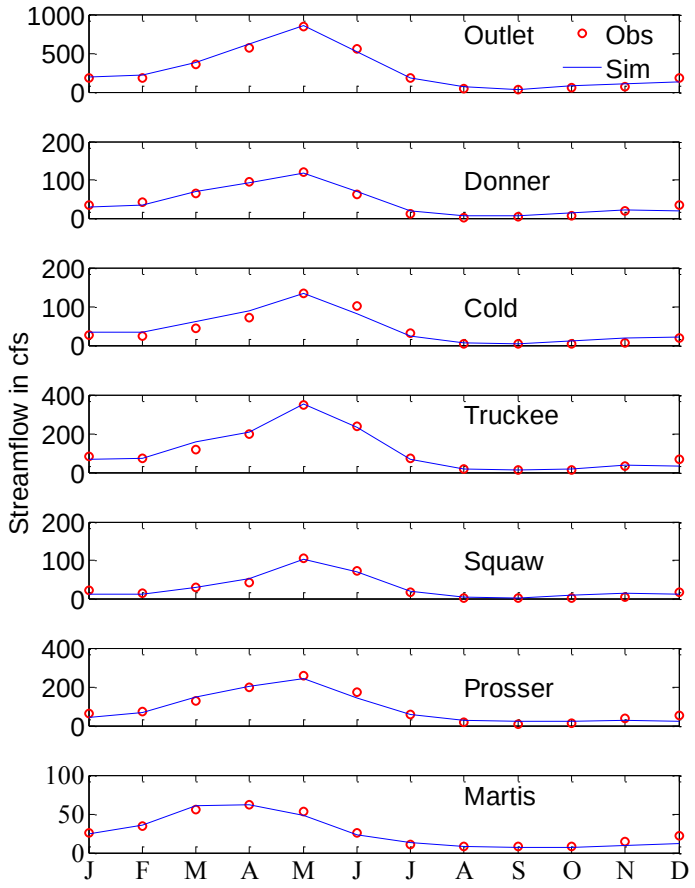

Figure 15: Observed vs. simulated mean monthly streamflows from PRMS (Huntington et al., 2013).

Figure 15 shows a good fit between simulated and observed mean monthly streamflow (1980-2011) for the basin outlet and sub-watersheds from the calibrated

PRMS model. For MODFLOW calibration, the ratio of mean recharge plus runoff to precipitation $\frac{\overline{RCH+RUNOFF}}{PPT}$ was adjusted so outflow from Lake Tahoe matched observed values. Hydraulic conductivities (K_h, K_v) were adjusted to match observed groundwater levels. The complex connectivity of the entire system caused assigned K values to be highly sensitive and unique. Calibrated hydraulic conductivities are within the range of silty sands and glacial outwash, according to Fetter (2001). Table 3 shows calibrated hydraulic conductivity values for each layer of the HFM. Figure 16 illustrates the goodness of fit between the simulated and observed groundwater heads.

Layer	Kh (m/d)	Kv (m/d)
1	4.20	4.20
2	3.60	3.60
3	5.30E-03	5.30E-03
4	1.00E-03	1.00E-03

Table 3: Calibrated vertical and horizontal hydraulic conductivities for each layer of the hydrogeologic framework model.

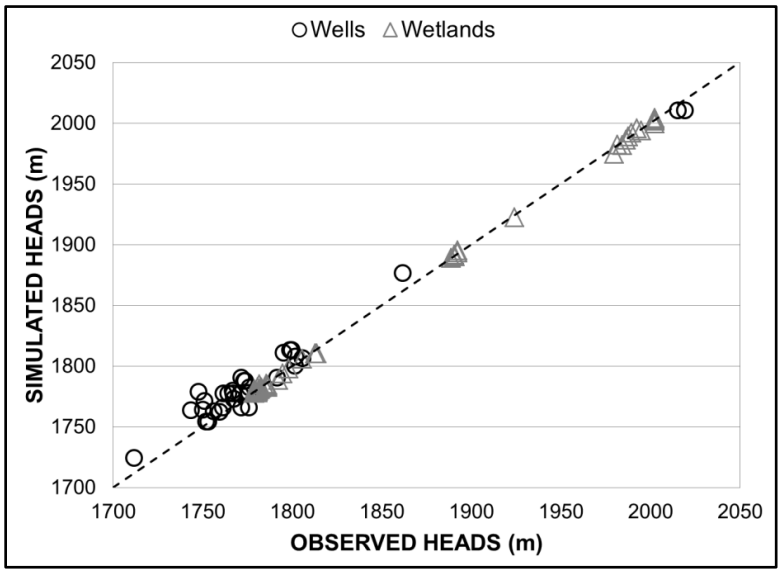

Figure 16: Calibrated, steady-state heads at wells and wetland areas show an excellent fit to observed values (Huntington et al., 2013).

The GSFLOW integrated model calibration consisted of matching streamflow in the Truckee River near the center of the watershed and at the outlet, water body stages in Donner Lake and Martis and Prosser Reservoirs, and monitoring well and wetland area heads. Daily discharge from Lake Tahoe, Donner Lake, and Prosser Reservoir are assigned to the stream segment immediately downstream of the water body. Figure 17 illustrates the goodness of fit between observed and simulated streamflow of the Truckee River at the gage near Truckee, CA from 2000 to 2010.

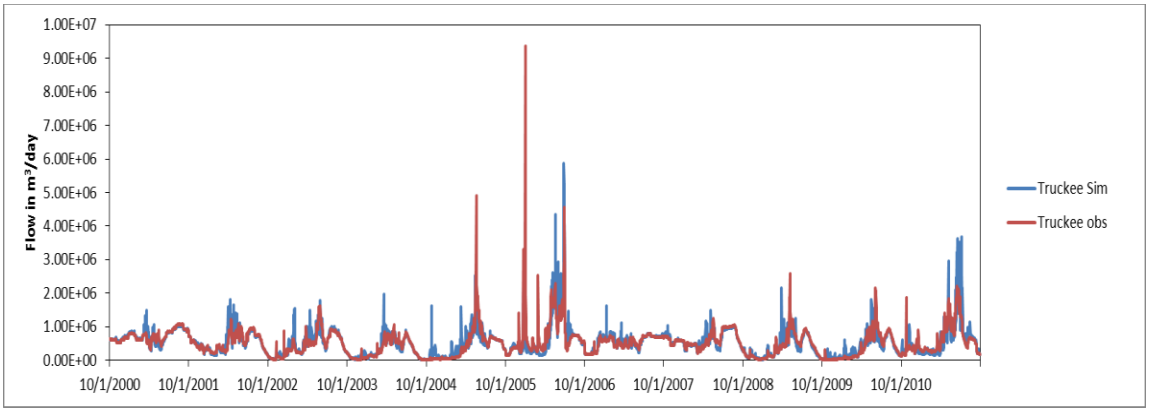

Figure 17: Observed vs. simulated streamflow for the Truckee River at Truckee, CA

Sensitivity analysis

Wetland locations were used to constrain the steady state calibration. Aquifer hydraulic conductivity (K) was tightly constrained, as illustrated by the sensitivity analyses shown in Figures 18 and 19. Spatial distributions of heads within 1 m of land surface were displayed for different horizontal and vertical K values scaled by a factor of 10. When decreased by a factor of 10, it is evident that the model over estimates head elevations (Figure 18a). When increased by a factor of 10, the model clearly under

estimated head elevations and did not simulate heads near known surface water areas (Figure 18b). The calibrated K distribution provides the most accurate representation of groundwater head levels (Figure 18c). Groundwater recharge sensitivity to changes of horizontal and vertical Ks was also observed. Figure 19 displays simulated recharge over a 2 year period with varying K values.

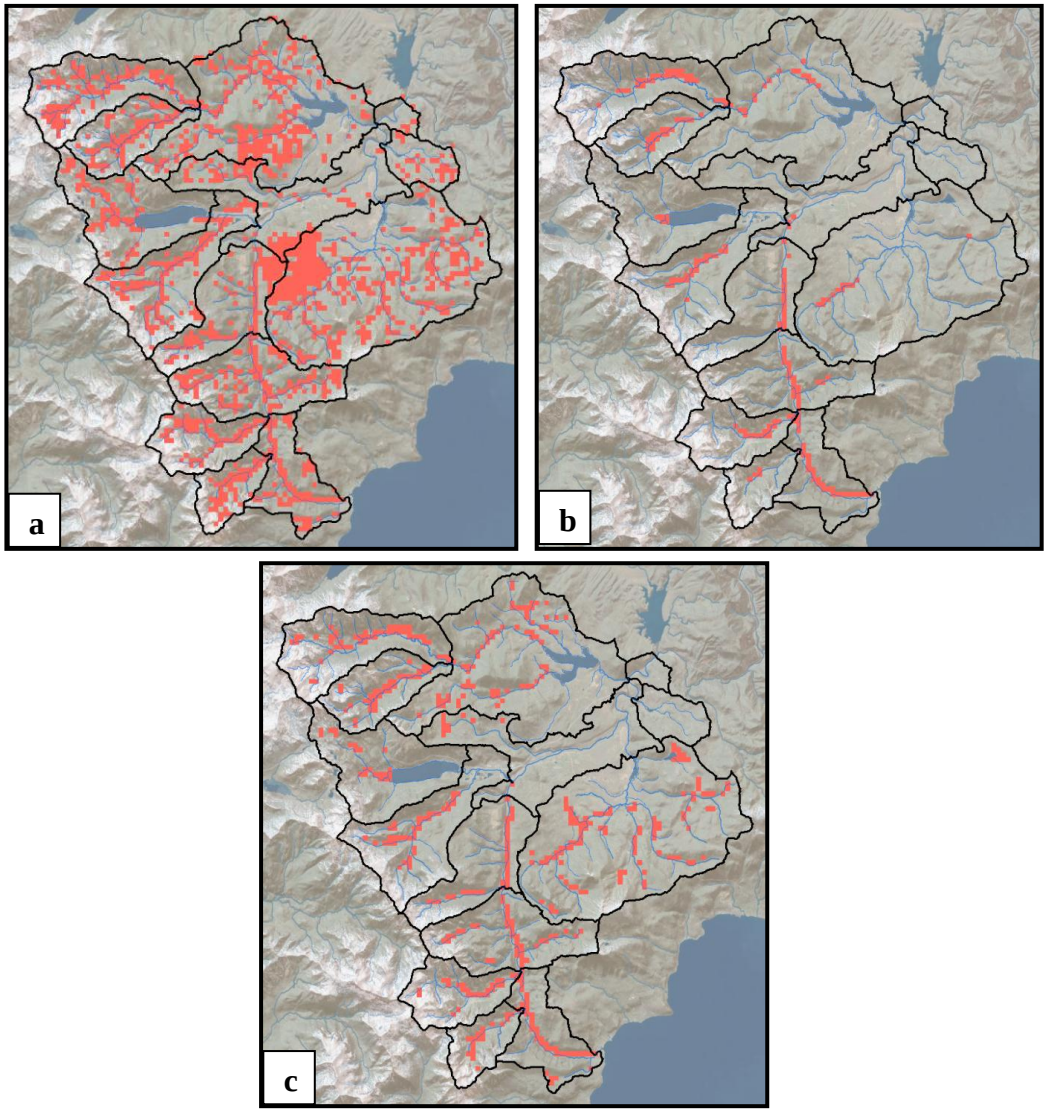

Figure 18: Spatial distribution of groundwater heads within 1 m of land surface shown in red where calibrated hydraulic conductivity values were (a) decreased by a factor of 10 and (b) increased by a factor of 10 for all layers. Optimally calibrated values (c) display heads that coincide with known near-surface water levels.

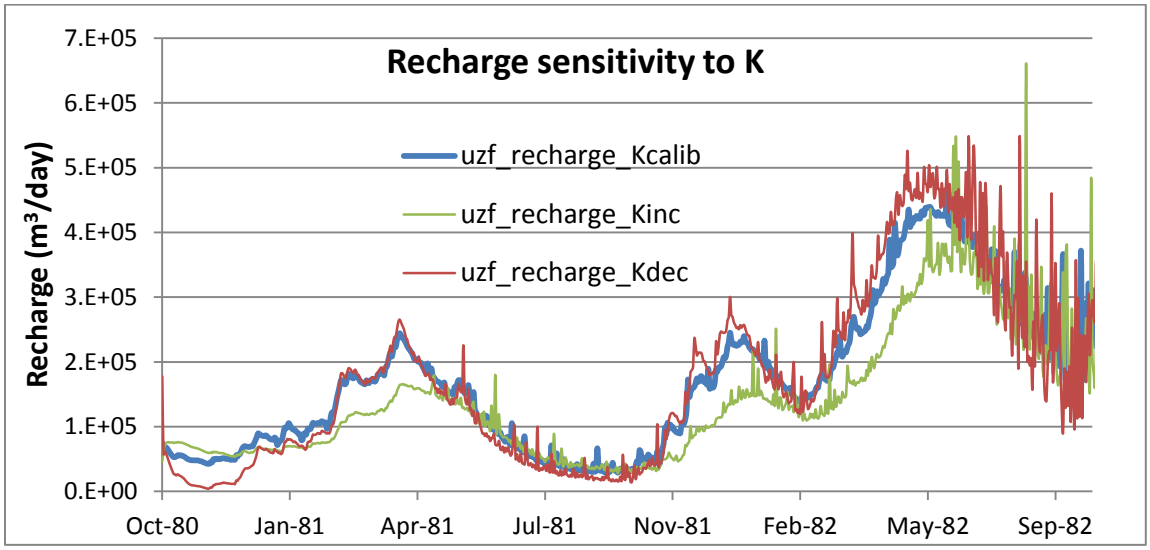

Figure 19: Recharge over two water years, given increases (Kinc) and decreases (Kdec) in horizontal and vertical K by a factor of ten. Recharge trends of the calibrated model are denoted by Kcalib.

Total daily groundwater recharge rates in Figure 19 did not increase proportionately to the increase in hydraulic conductivity. Contrastingly, the low K distribution (red line in Figure 19) showed highest recharge rates along the climbing limb of recharge periods, while the high K distribution caused the lowest recharge rates during these periods. The medium K distribution, or the calibrated values of K, were only observed to cause slightly higher recharge rates during baseflow periods (July – Nov 1981, Figure 19), and otherwise generally maintained rates between the high and low K distributions.

Groundwater Flow Directions

After model calibration and sensitivity analyses, groundwater head elevations were extracted from the steady state-model for each hydrogeologic layer. The Martis

Valley head gradients generally mimicked topography, which is typical for mountainous watersheds. Contour lines of head elevations were created in GIS and used to determine the horizontal component of flow; groundwater flow directions are perpendicular to the head contours (Fetter, 2001). The general flow directions for the Martis watershed were inferred from a 50 m interval contour map derived from the simulated heads (Figure 20). Temporal groundwater head fluctuations within the upper two layers were observed, so layer 3 (weathered bedrock) was used to derive the contours. Layer 3 also provides continuous head measurements across the model domain, unlike layers 1 and 2, which are spatially discontinuous.

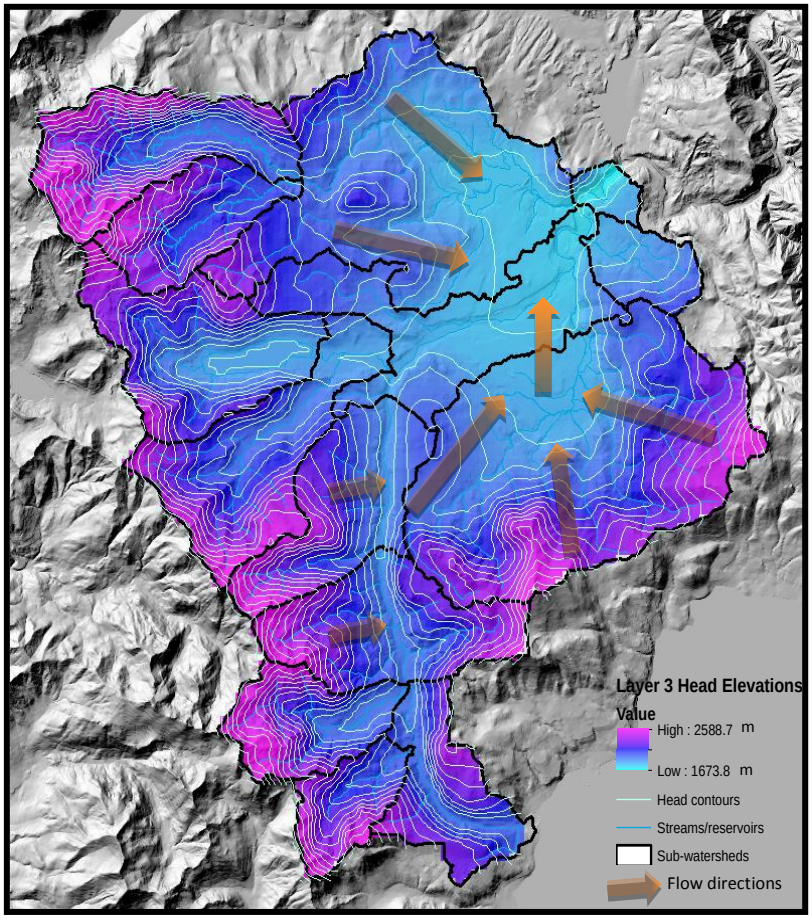

Figure 20: General groundwater flow directions inferred from simulated head elevations in layer 3. Groundwater gradients typically mimic topography.

Based on the flow lines inferred from the head elevation contours, groundwater from the northern section of the watershed moves south and east before discharging to the Truckee River and leaving the basin. Groundwater originating in the sub-basins along the south-western portion of the watershed flows directly east towards the north trending Truckee River. The south side of the watershed shows groundwater converging into the Martis Creek sub-basin where it is directed north towards the Truckee River once in the main valley. The eastern slopes direct the groundwater northwest where it likely mixes with groundwater from the south and west before discharging into the river. The results from the steady state GSFLOW modeled heads are consistent with the conceptual model of groundwater flow.

Model-Stable Isotope Comparison

Modeled simulations were coupled with isotopic measurements from 2012 to investigate relationships between snowmelt and streamflow and evaluate model-geochemistry compatibility. As previously discussed, isotopic ratios evolve as the snowpack undergoes physical and chemical changes, causing isotope fractionation. This is generally seen as lighter (more depleted) isotopes sublimate, melt, and evaporate from the snowpack, causing the remaining snow to become isotopically heavier (more enriched) over time. Under this premise, it can be expected that snow samples will yield enriched (less negative) isotopic measurements after significant snowmelt has taken place. Snowmelt trends can be observed in the isotopic data from the Martis Creek snowmelt in Figure 21.

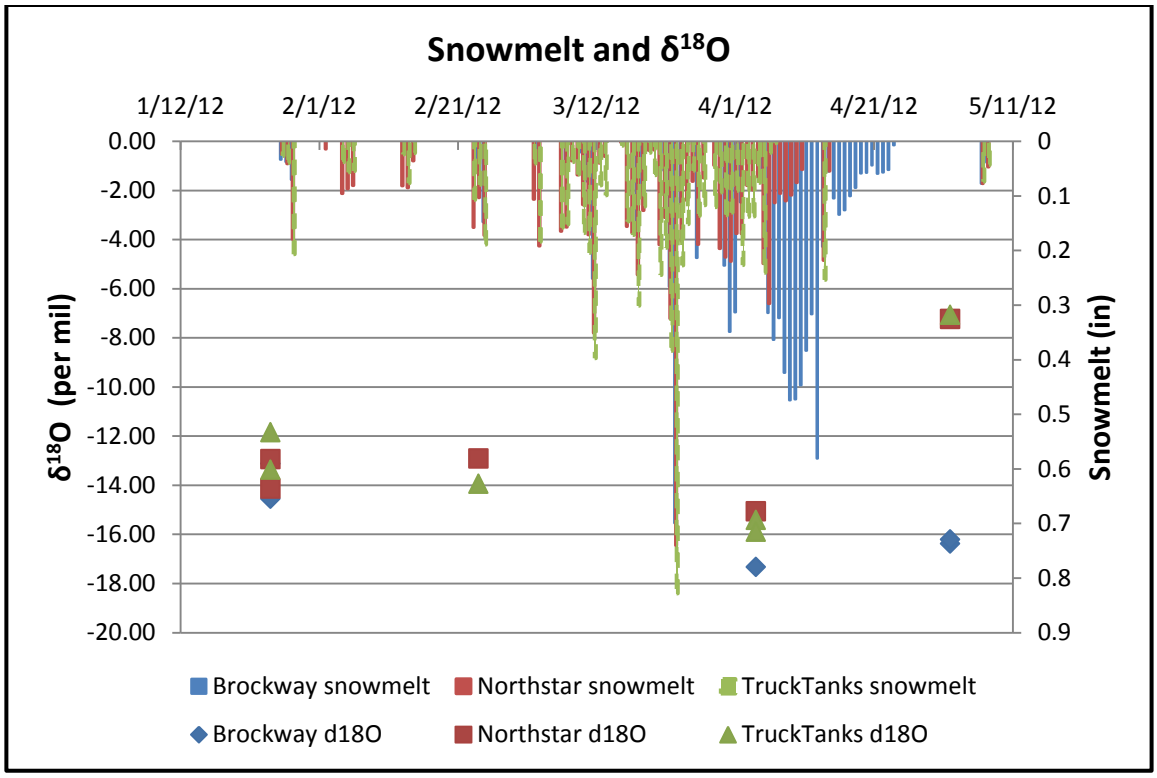

Figure 21: Time series of deuterium evolution as snowmelt occurs from three sites within the Martis Creek sub-watershed. The snowmelt displayed from the top of the chart is simulated by the model at the three locations of isotopic sampling.

The snowmelt hydrograph presented in Figure 21 was generated from the GSFLOW model and represents snowmelt magnitude over time from the grid cell corresponding to each sample site. The majority of melt occurs after the end of March, wherein the measurements become isotopically heavier (the final samples), as expected. Isotopic depletion of the samples in April, before the post-snowmelt enrichment trend, is an unexpected result.

Once snowmelt reaches the stream channels as overland flow, hydrographs will increase to reflect this melt water pulse. Stable isotope measurements from two forks of Martis Creek were compared to modeled streamflow at the convergence of the two forks (Figure 22).

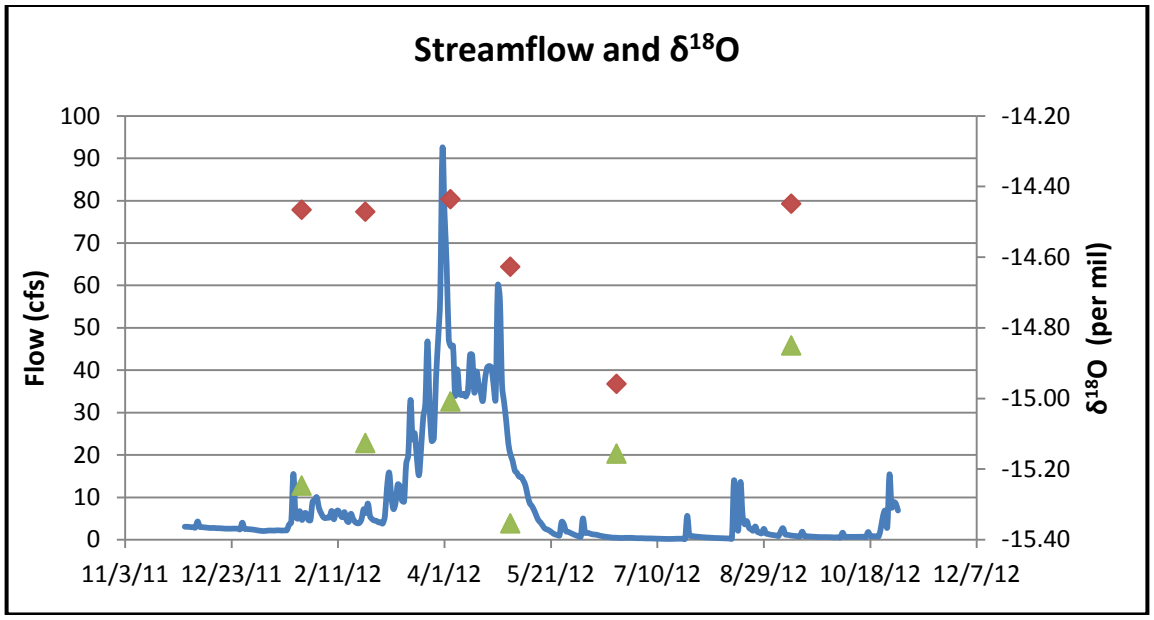

Figure 22: The main stem of Martis Creek $\delta^{18}O$ represented by red diamonds and the east stem $\delta^{18}O$ represented by the green triangles. The blue line is the simulated hydrograph at the convergence of the main and east forks.

The hydrograph shows peak flows through the month of April, while the isotopic values of the stream water show a relative lag before the more negative melt water signal appears. The most depleted signal from the east stem (green triangles in Figure 22) is measured in early May, while the most depleted signature in the main stem (red diamonds) of Martis Creek does not occur until mid-June, well into the baseflow period.

Groundwater Recharge

The GSFLOW model simulates groundwater recharge for each grid cell at a daily time step by accounting for vertical flow through the unsaturated zone. One output file of the GSFLOW model contains basin wide simulation results for each time step, including the UZF recharge values. These values were compared to the PRISM precipitation to observe annual relationships and compute recharge efficiency. Figure 23 shows that

annual recharge variations correlate to annual precipitation trends. Annual groundwater recharge is clearly a function of annual precipitation, yet temporal lags can be observed in the response of recharge to precipitation. For example, the largest precipitation year of the simulation period is 1982, whereas the largest recharge spike is not seen until 1983.

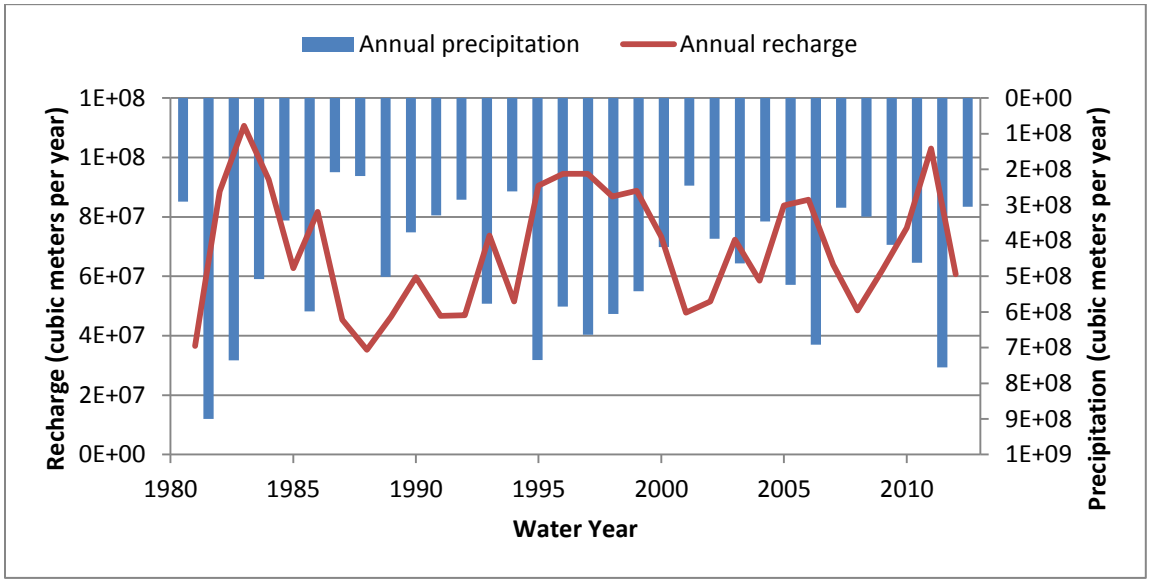

Figure 23: Annual recharge rates overlaying annual precipitation rates for the entire watershed; based on the GSFLOW distribution of precipitation and UZF package calculated groundwater recharge.

Recharge estimates rely on indirect measurements, whereas precipitation can be measured directly. Thus, applying a recharge efficiency, computed as the ratio of annual recharge to annual precipitation, is an effective tool for quantifying a basin wide relationship between precipitation and recharge and estimating the recharge component of the water budget when other resources are unavailable. Figure 24a shows annual recharge efficiency variations of the Martis Valley watershed. Figure 24b displays the trend of recharge efficiency with increasing precipitation. Recharge efficiency does not increase with precipitation; rather, it appears to have a slight decreasing trend. Although

recharge rates are clearly a function of precipitation as seen in Figure 23, recharge efficiency seems to be driven by different parameters.

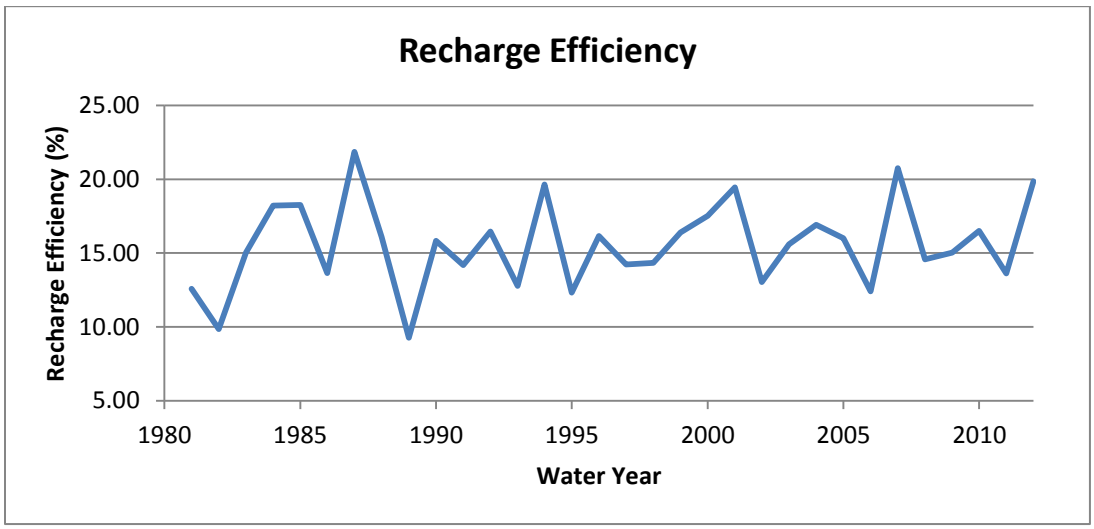

Figure 24a: Values of annual recharge efficiency, or percentage of precipitation that becomes recharge. Mean recharge efficiency is 15.6%.

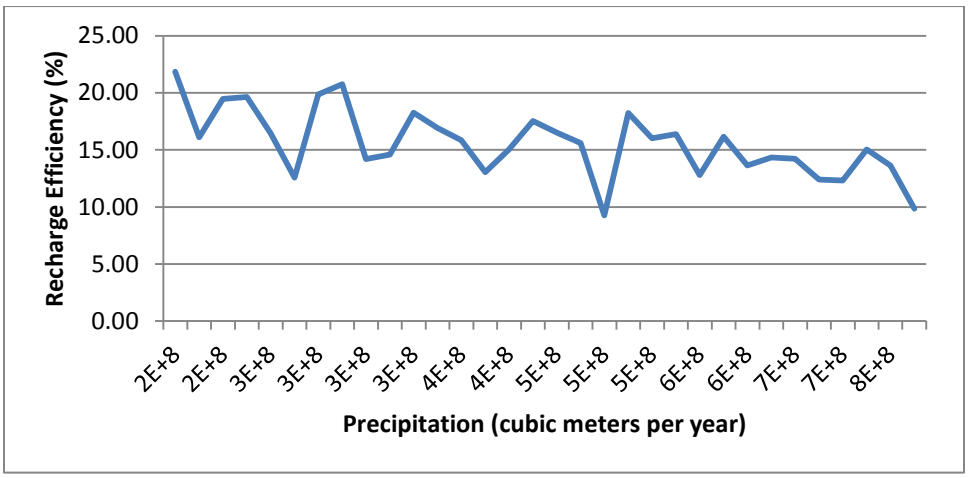

Figure 24b: Trend of recharge efficiency with increasing precipitation.

Mean groundwater recharge rates (m^3/d) were extracted from the model simulation and plotted in GIS for mean annual (Figure 25) and mean monthly (Figure 26) rates at each model grid cell. Visualization of the simulated data allowed for

spatiotemporal analysis of recharge at basin and sub-basin scales. Simulated mean annual recharge magnitudes and locations were compared to previous water budget recharge estimations and geochemical investigations, respectively. In the following figures, low to high recharge is represented by light orange to blue, respectively.

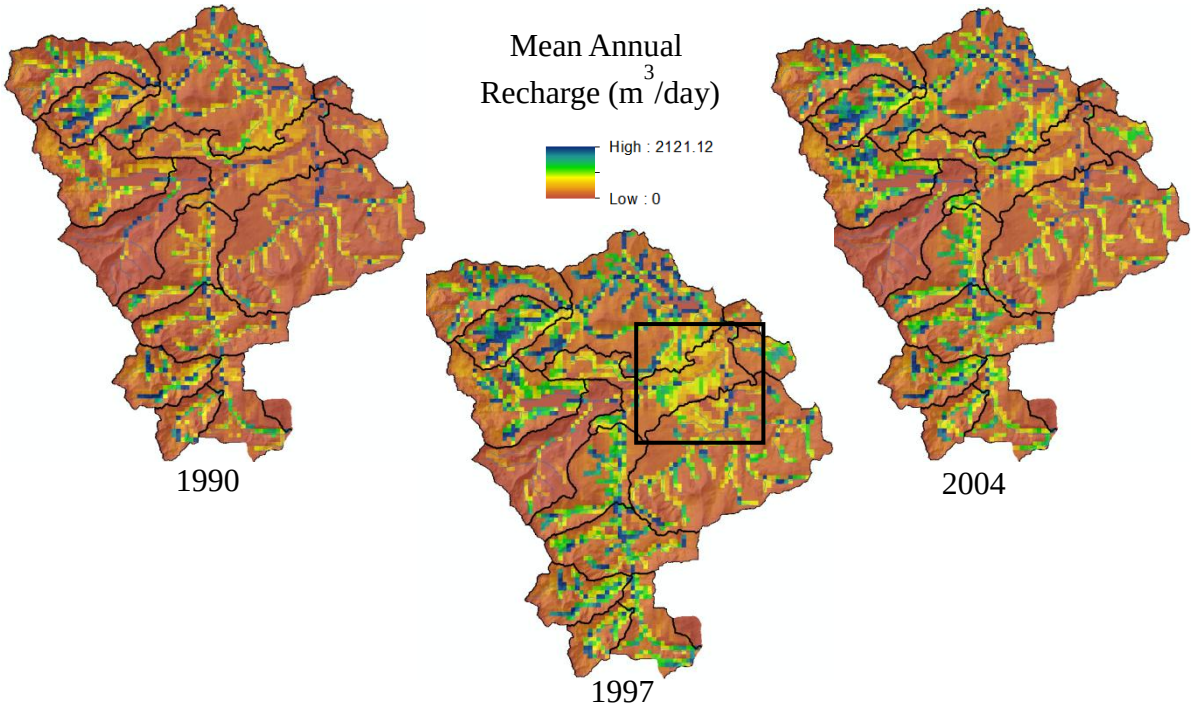

Figure 25: Simulated mean annual groundwater recharge for three water years: 1990, a below average precipitation year; 1997, an above average water year; and 2004, an average year. Recharge zones are light orange to blue. The black square shows the general location of the central Martis Valley groundwater basin area.

The GSFLOW model consistently simulates the highest recharge rates near stream channels, and also accentuates recharge in valley areas. Both of these high recharge zones coincide with high water table levels. Mean annual recharge for 1997, an above average precipitation year, emphasizes high recharge throughout stream channel and upland alluvial areas, while also displaying significant recharge in areas of central Martis Valley (black square). In contrast, mean annual recharge for 1990, a below

average precipitation year, shows little upper elevation recharge and highlights only stream channel and central valley recharge. The average water year 2004 emphasizes mainly stream channel and Martis Valley recharge, with some upper elevation recharge occurring in alluvial valleys of sub-basins.

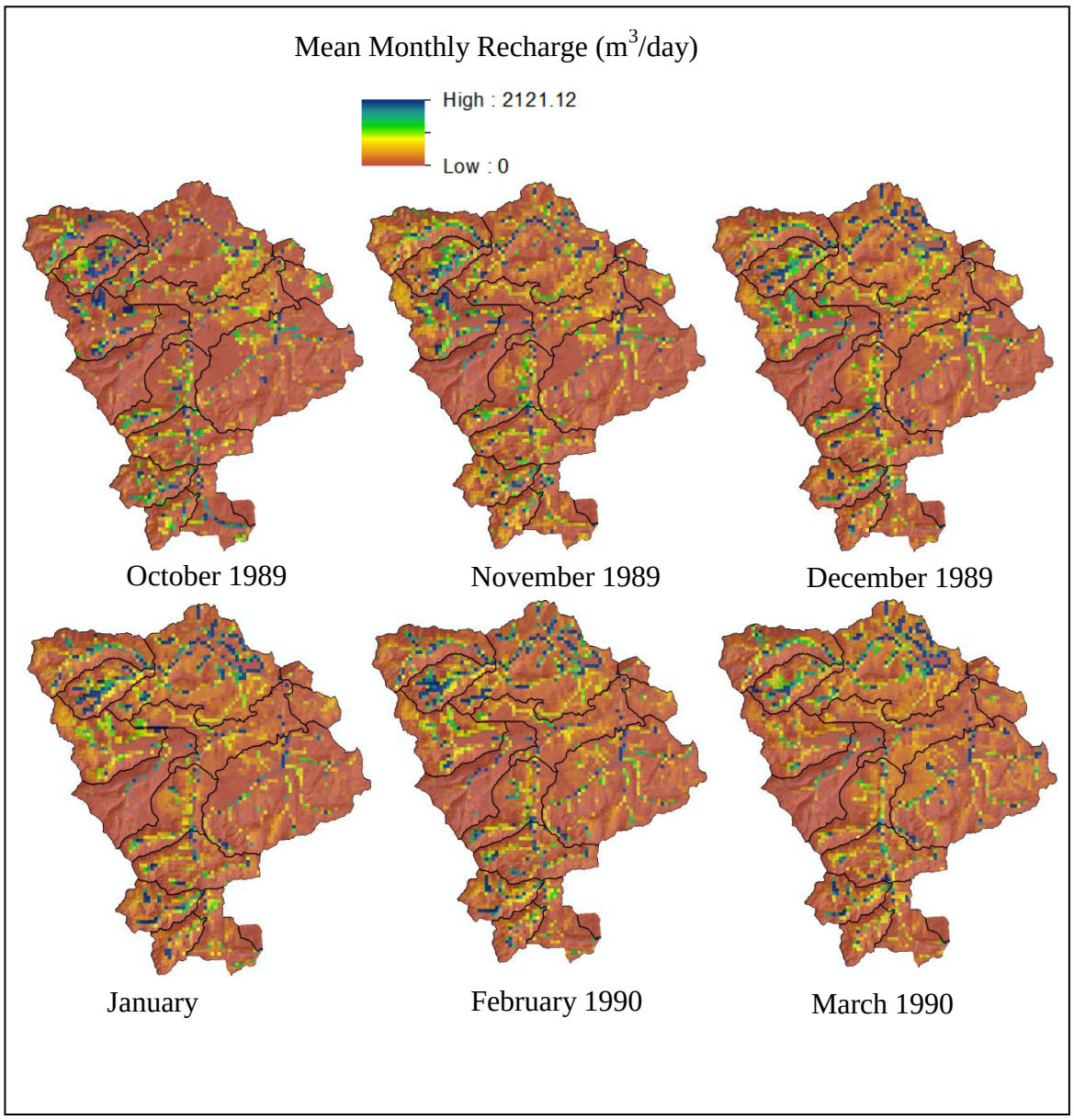

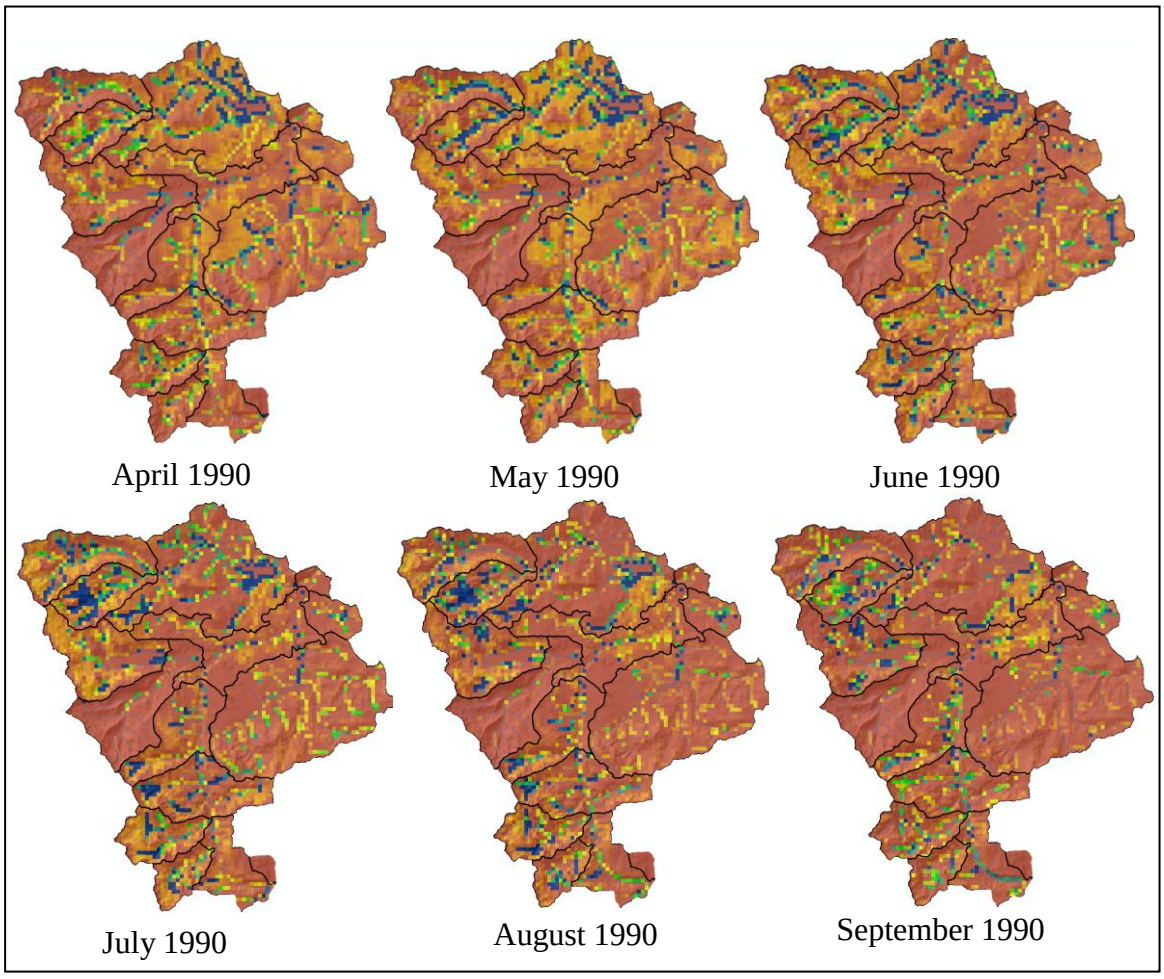

Figure 26: Mean monthly groundwater recharge for water year 1990, illustrating seasonal variations in location and magnitude. Low to high recharge is displayed as light orange to blue, respectively.

Mean monthly recharge maps illustrate seasonal fluxes. Water year 1990 was chosen because it was a near average year for precipitation and highlights general annual recharge trends seen in the Martis basin. During the beginning and end of the water year, recharge is focused near some stream channels and in central valley areas. As the water year progresses, recharge shifts towards upper elevations during winter months where it is limited to stream channels, and then migrates back down slope during spring. High recharge rates are observed in the northern sub-basins during spring, while the trend

shifts to western sub-basins during summer months. An interesting result is seen between the months of May and June. May recharge is heaviest throughout the watershed, including low elevation areas, while June displays little recharge in the low elevations and highlights more mid to upper elevation recharge. This is not seen in all years, as shown in Figure 27, which focuses on the springtime (April-June) recharge fluxes of different years.

Spring recharge fluctuations in Figure 27 show variable peak recharge months. All three years are above average water years. In 1984, the watershed receives most recharge in April, while following May and June show recharge retracting to stream channel areas. The 1996 maps also display heavy recharge in April, and show May and June continuing with high recharge rates. In 2006, recharge peaks in May and carries on through June, while very little recharge occurs in April. These variations clearly emphasize recharge processes as highly sensitive to seasonal fluctuations in precipitation and temperature.

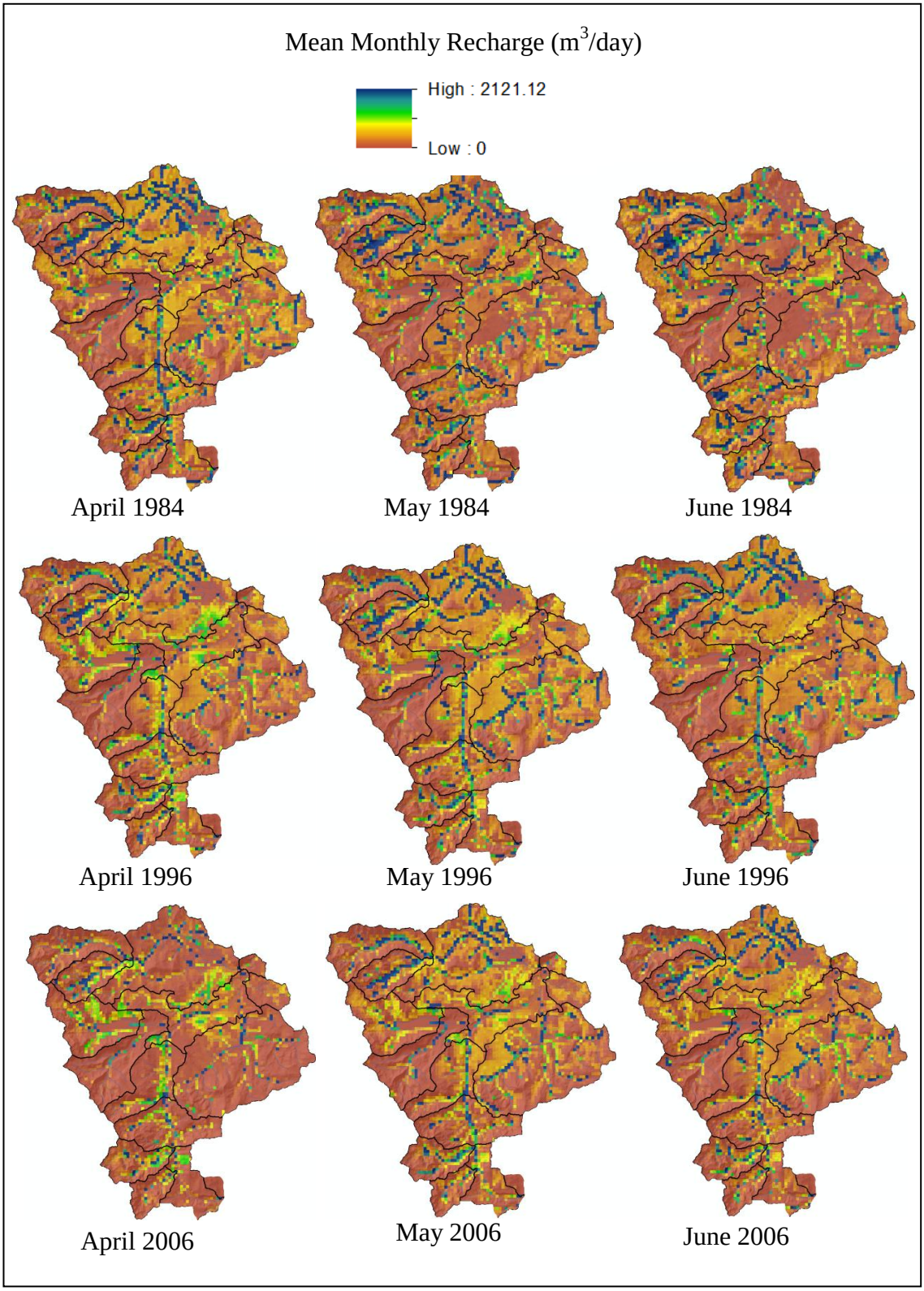

Figure 27: Spring recharge fluxes for three above average precipitation years.

Numerical modeling presents the opportunity to estimate groundwater recharge locations and magnitudes over a simulation period of several years, therefore eliminating seasonal anomalies and illustrating more stable trends. Figure 28 presents mean annual recharge over the entire simulation period (October 1, 1980 – September 30, 2012).

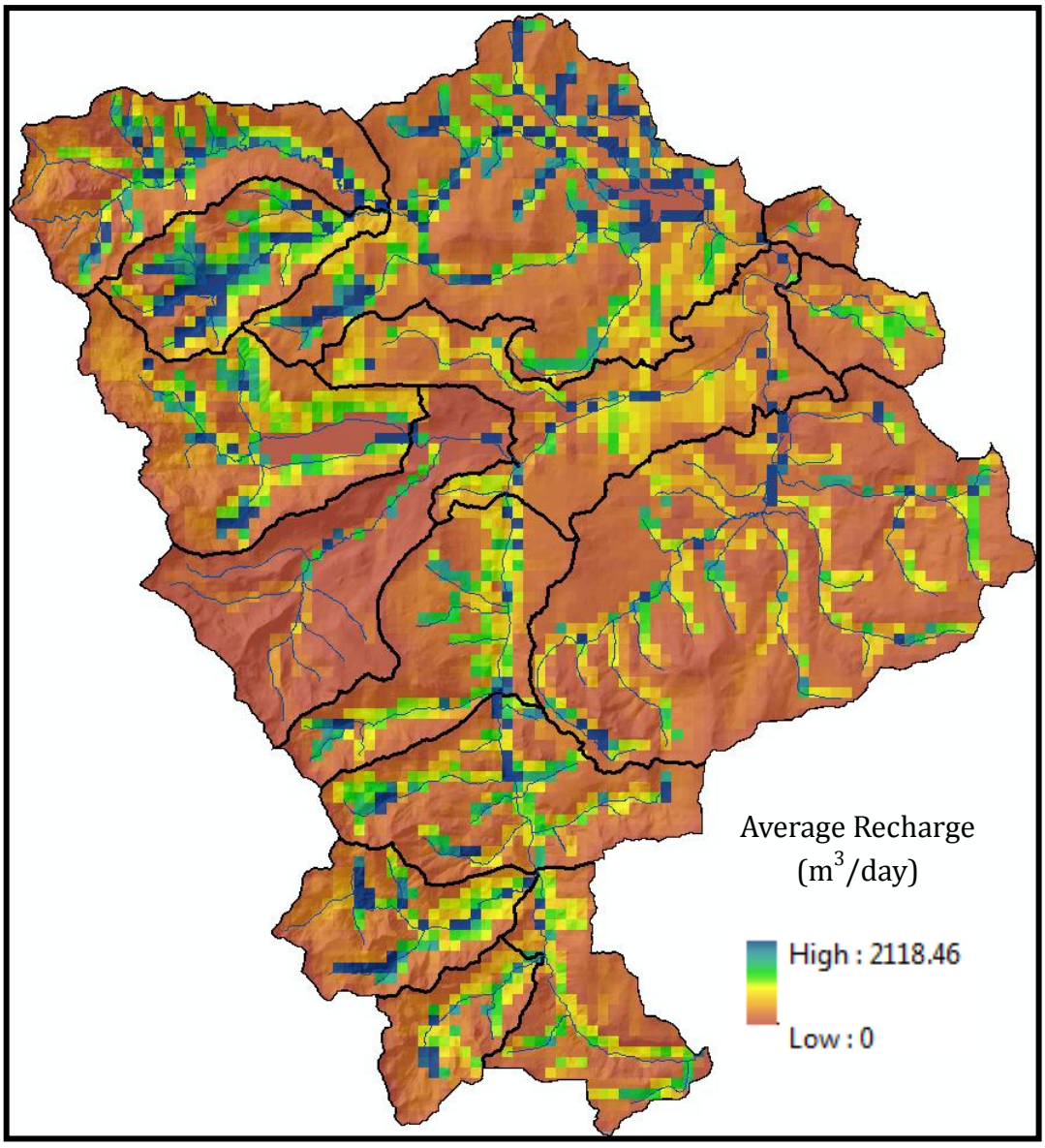

Figure 28: Mean annual recharge in cubic meters per day over the model simulation period, highlighting principal recharge zones and relative magnitudes.

It is clear in Figure 28 that recharge largely occurs along stream channels and valley areas where the water table is nearest to the surface. To observe and quantify recharge as a function of elevation, the watershed was subdivided into three levels: below 1800 m, 1800 m to 2050 m, and above 2050 m. The 1800 m contour was chosen to represent the extent of the valley floor area and was based on aerial photographs. The mid-range zone (1800 m – 2050 m) was chosen to represent the mountain block-alluvium interface, and the portion above 2050 m extends to the watershed boundary and includes the upper elevation mountainous region. Figure 29 displays these elevational watershed subdivisions.

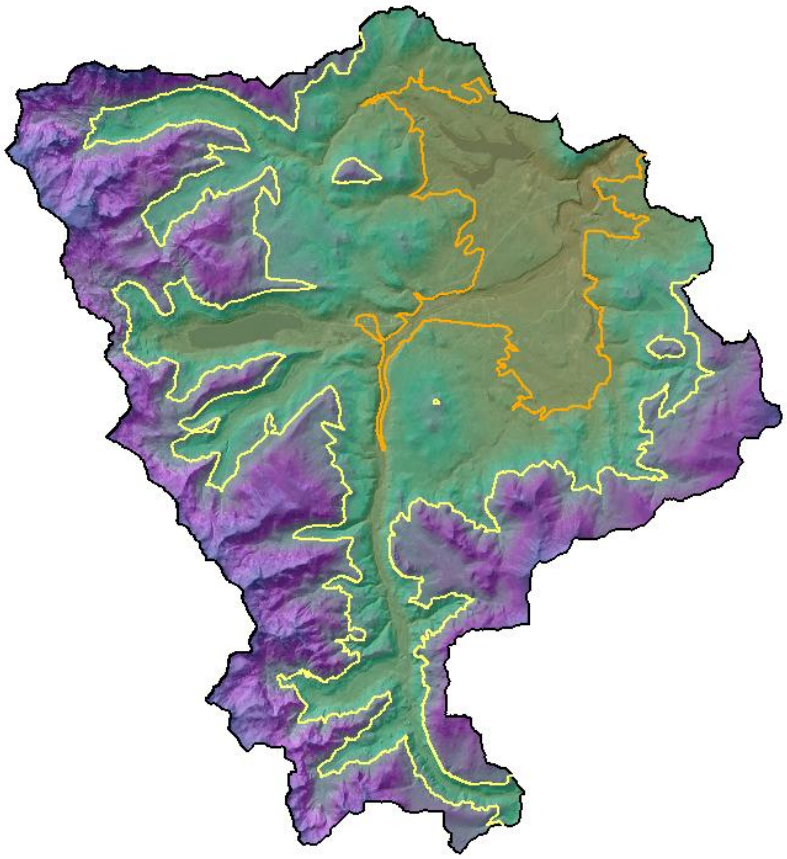

Figure 29: Three designated elevation zones: Below 1800m (brownish tint outlined in orange), above 1800 m and below 2050 m, (green hue outlined in yellow), and above 2050 m, (blue to purple coloring).

Recharge volumes were computed for each elevational subdivision, and normalized by the section area. The area below 1800 m contributes approximately 14.8 million cubic meters annual recharge, areas between 1800 m and 2050 m contribute 37 million cubic meters annually, and regions above 2050 m contribute 18.5 million cubic meters of recharge per year. These values, along with the normalized rates and recharge efficiencies, are given in Table 4.

	Below 1800 m	1800 m-2050 m	Above 2050 m
Average Recharge (m^3/yr)	1.48E+07	3.70E+07	1.85E+07
Area (m^2)	8.10E+07	2.30E+08	1.80E+08
Percent Total Area (%)	16.5	46.8	36.7
Percent Total Recharge (%)	21	53	26
Normalized Recharge Rates (m/yr)	0.24	0.19	0.13
Recharge Efficiency (%)	30.3	16.8	9.1

Table 4: Mean annual recharge rates per elevation-based section, along with area and percent of total area of each section. Recharge amounts were divided by the section area to compute normalized rates, and recharge efficiency was computed based on mean annual precipitation within each portion.

The portion of the watershed below 1800 m, consisting of the principal valley floor area, has the highest normalized recharge rate, followed closely by the 1800 m – 2050 m portion. These two areas contribute roughly 75% of annual recharge amounts. The recharge occurring in the elevations above 2050 m is concentrated along the few stream channel and alluvial areas, causing the recharge efficiency to be very low. Figure

30 illustrates the decrease in groundwater recharge as elevation increases. The highest recharge rates occur at the lowest elevations where the water table is nearest to the surface. The mid-range elevations, largely consisting of the mountain block-alluvium interface, sustain significant recharge rates. Beyond 2100 m, into the mountain block, recharge rates drop significantly.

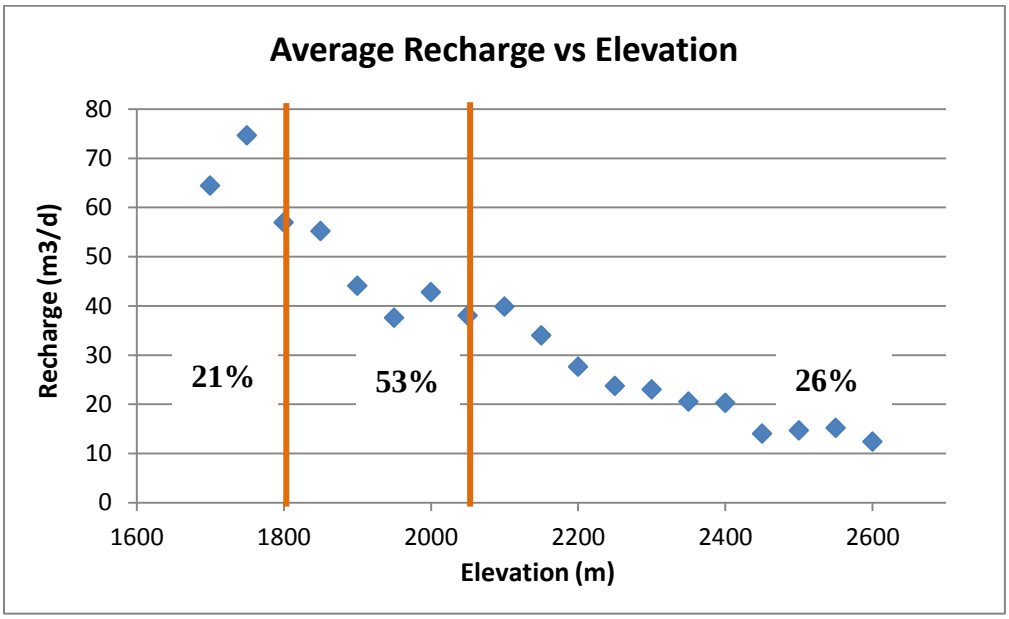

Figure 30: Trend of average recharge rates with increasing elevation. Mean daily recharge rates from the simulation period were averaged over 50 m elevation intervals. Percentages of total recharge are shown for each elevation-based section, divided by orange lines.

Total average annual recharge estimated from the GSFLOW model is 70.3 million cubic meters (57,000 ac-ft) for the entire watershed. It is clear that the low to mid-range elevations contribute the majority of recharge, but the higher elevations do contribute recharge where alluvial areas and near-surface water table conditions exist. To further evaluate spatial recharge distribution, recharge within each sub-basin was

computed. Sub-basin recharge contributions were calculated based on the mean annual values illustrated in Figure 28. Figure 31 shows the fourteen sub-basins that make up the Martis watershed, and their average annual recharge contributions, along with recharge rates normalized by sub-basin area, are presented in Table 5.

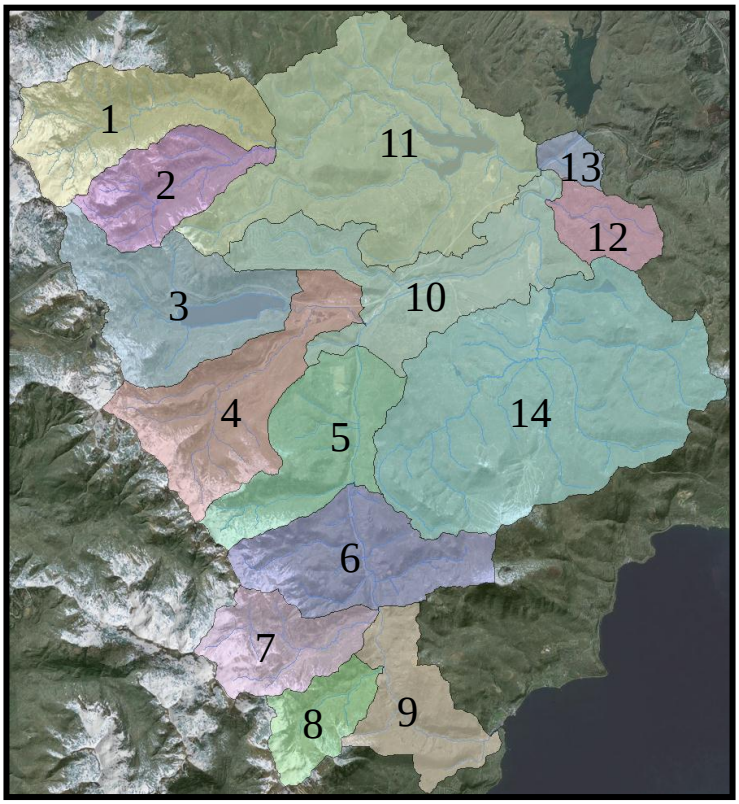

Figure 31: The fourteen sub-basins of the Martis Valley watershed.

The largest three sub-basins (10, 11, 14), contribute roughly half of the total annual recharge. As seen in Figure 31, these three sub-basins include the downstream and largest valley areas in the watershed. These areas were the main focus of previous recharge estimations. The remaining sub-basins have smaller total areas, less extensive stream networks, and smaller alluvial areas to accumulate recharge. However, significant

annual recharge is accumulated from these sub-basin contributions. Table 5 presents each individual sub-basin mean annual recharge contributions.

Average recharge (m^3/yr)	Sub-basin number	Normalized Recharge (m/yr)
3.15E+05	13	7.28E-02
1.39E+06	12	1.23E-01
1.82E+06	4	4.72E-02
2.19E+06	8	1.6E-01
3.32E+06	9	1.46E-01
4.31E+06	7	2.08E-01
5.40E+06	5	1.70E-01
5.90E+06	1	1.72E-01
6.05E+06	6	1.75E-01
6.39E+06	3	1.68E-01
6.88E+06	2	3.17E-01
8.34E+06	10	1.89E-01
1.20E+07	14	1.17E-01
2.07E+07	11	2.48E-01

Table 5: Mean annual recharge from each sub-basin within the Martis watershed. Values are listed from smallest to largest, with corresponding sub-basin number. Normalized recharge rates were computed by dividing the average recharge by the area of the corresponding sub-basin.

Discussion

Previous Work

Previous water budget based recharge estimations in Martis Valley relied on 'recharge efficiency' coefficients to compute recharge rates from annual precipitation amounts. The water balance equations applied for these estimations required several assumptions (i.e. evapotranspiration) and relied on instantaneous streamflow measurements. Thus, estimations of recharge were highly varied. Hydro-Search Inc. (1995) estimated annual recharge of 18,179 ac-ft. Nimbus Engineers (2001) estimated a recharge of 23,744 ac-ft/yr. Interflow Hydrology and Cordilleran Hydrology, Inc. (2003) estimated 34,560 ac-ft annual recharge, and Seshadri et al. (2012) estimated a mean annual recharge of 32,745 ac-ft. These previous investigations estimated recharge for several sub-sections of the watershed, assumed to each contain homogenous hydrologic properties. Attempts were made to account for water that was considered to recharge a sub-section, but later discharge from a down gradient section. However, these interconnected fluctuations are extremely difficult to measure and/or estimate. Recharge estimations were focused within the "Martis Valley Groundwater Basin" (MVGB) designated by Hydro Search Inc. (1974), shown in Figure 32. The MVGB covers the majority of the principal sub-basins, but does not encompass any of the sub-basins to the west, causing underestimations. Based on the GSFLOW estimations, the average recharge contributed by the sub-basins that make up the MVGB is approximately 41 million cubic meters per year (33,000 ac-ft/yr), which is in the range of previous estimations.

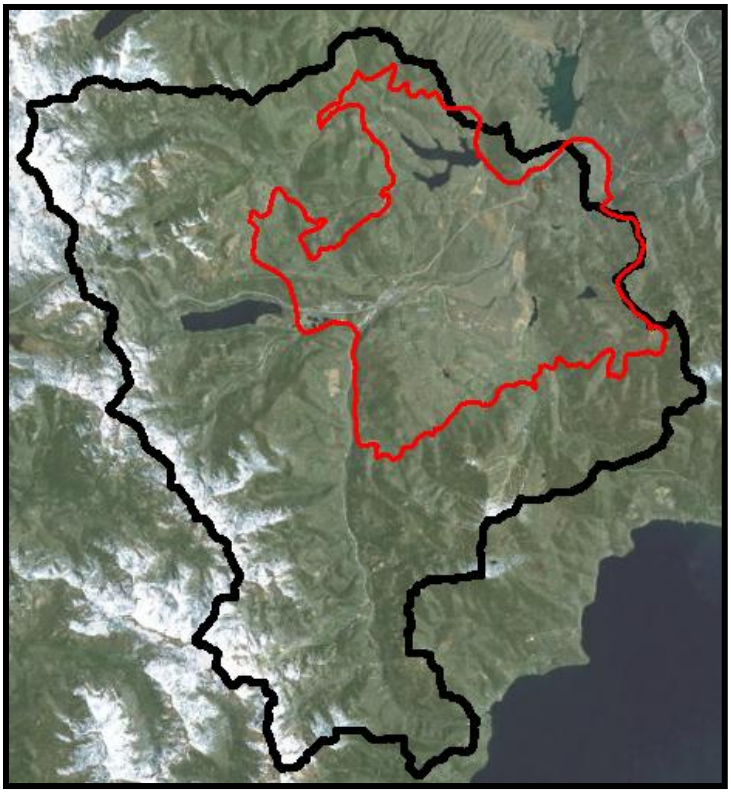

Figure 32: Martis watershed and model domain (black line), overlain by the MVGB border (red line), designated by Hydro Search, Inc (1974) and used in subsequent recharge investigations.

The geochemical techniques applied by LLNL (Singleton and Moran, 2010; Segal, 2013) and summarized in this report produced relative spatial variations and general conceptualizations regarding the recharge processes in the Squaw Valley and Martis Creek sub-watersheds. The significance of low and mid elevation recharge and infiltration through unconsolidated alluvial and valley floor sediments was emphasized. These results were based off sampling conducted within available wells and surface water sites in each study area. These spatial estimations of recharge in Martis Valley avoided the interconnectivity complications faced by water budget estimations and broadly captured final recharge stage within each sub-basin. These methods were more directly

focused on final recharge locations rather than forming section-by-section estimates. The emphasis placed on groundwater recharge occurring below 2050 m elevation has been supplemented by findings of this research. Results from this report allow for quantifications of these spatial estimations.

Baseflow Analysis

Minimal baseflow response to precipitation after consecutive dry years indicates that depleted alluvial aquifers must be recharged to a certain level before it is able to discharge to streamflow. High streamflow after consecutive low precipitation years may also impede groundwater discharge when stream stage is above the water table. The Martis Valley aquifer appears to require 2-3 consecutive average to above average precipitation years for baseflow to respond to precipitation. In years following consecutive below average precipitation years, baseflow is not highly indicative of recharge.

The recharge and streamflow percentages of precipitation calculated for the Martis Creek sub-basin represent annual averages, and therefore do not capture variations within a shorter (seasonal) period. The portion of precipitation that was designated as baseflow was a close estimation to recharge efficiency calculated from model results. This similarity supports both methodologies for evaluating recharge percentage of precipitation. The results highlight the highly variable and sensitive nature of baseflow, and thus recharge, in Martis Valley.

Stable Isotope Analysis

The isotopic data available for analysis was sparse and only used for basic conceptualizations. Additional samples throughout the watershed over a longer period of time would be necessary to form more quantitative conclusions. Summer precipitation and groundwater samples from each season would strengthen the investigation. It was clear that spring streamflow samples carried the snowmelt isotopic signatures. Summer streamflow contained a heavier isotopic influence. This is likely a combination of late season snowmelt, summer rain events, and lake discharge, all of which carry heavier isotopic signals relative to mid-winter precipitation. Sublimation effects observed from the GMWL graph supplemented the preliminary isotopic relationships regarding snowpack evolution.

Sensitivity Analysis

The effects of varying horizontal and vertical hydraulic conductivities (K_h, K_v) on groundwater heads were very clear. Increasing the K values dropped the groundwater levels below many areas of known near-surface and surface water, while decreasing Ks distributed groundwater within 1 m and above the surface over several dry areas of the watershed. The analysis confirms the hydraulic conductivities applied to the GSFLOW model were reasonable.

Groundwater recharge was also sensitive to variations in K values, but less intuitively than the head levels. Less recharge simulated with an increase in K could likely be a result of the high K values producing a greater unsaturated zone thickness causing attenuation of the infiltrating water. Accordingly, the lower K distribution

caused higher recharge rates during peak snowmelt periods, likely due to thinning of the unsaturated zone.

Groundwater Flow Directions

The flow directions inferred by Segal (2013) are based on geochemical data from a single year, whereas the flow directions based on modeled results are inferred from a steady-state condition, which represents more average circumstances. Slight differences in the results are inherent to the differing methods. In both cases, however, groundwater flow was found to generally mimic topography. The two separate methods form similar conclusions that solidify conceptualizations of groundwater flow directions, and provide a check for each methodology.

Model-Stable Isotope Analysis

Understanding isotopic evolution of a snowpack is important for sampling from a downstream location when attempting to trace the isotopic precipitation signal in streamflow, especially if sampling in the spring or summer. The anomalous isotopic depletion of snow samples in April could be attributed to late season precipitation from the north pacific (colder, more depleted), causing the samples to be relatively more depleted compared to the previous samples, which likely consisted of precipitation from the south pacific (warmer, more enriched). Because the sampling process consisted of capturing snowmelt from the bottom of the snowpack, a single event would not usually shift the isotopic signatures greatly. However, late in the season, with little snowpack remaining, a cold storm could essentially effect the entire snowmelt signal. A look into

the weather archives revealed that a cold front in early April did in fact deposit significant snowfall. This is likely the reason for the late winter depletion trend seen at all three sampling sites. Shortly after this anomalous cold event, the weather warmed drastically, causing the majority of melting to occur at the highest elevation site (Brockway summit), and the final snow samples to reflect the warming trend.

The temporal lag in a cold isotopic signature in streamflow makes conceptual sense as the earliest melt likely originates from lower elevations that carry a more enriched (warmer) isotopic signature than that of the higher elevations. It would take some time for the coldest signal to reach the valley stream sampling location. Although the measurements of Martis Creek (main) do trend lighter during peak runoff season, it is interesting to see the most depleted signal appear so late. This would suggest a few possibilities: 1) A portion of snowmelt infiltrates shallow soils and slowly passes to the stream as interflow. 2) Short groundwater flow paths contribute the cold signal of that season's precipitation. 3) The 2012 isotopic signals of winter precipitation were enriched compared to the groundwater background signal, essentially causing the baseflow signal to be more depleted than the 2012 runoff. A combination of these three interpretations is possible. However, since the same observation is not apparent in both forks of Martis Creek, and more data is not available, it is difficult to discern the exact cause.

The stable isotope time series overlain with simulated snowmelt and streamflow hydrographs illustrate relationships that enhance the Martis basin conceptual model. Snowpack enrichment occurs as the melt season progresses, but precipitation events late in the season can affect the snowmelt signature if relative snowpack amounts favor the event signal. Snowmelt runoff is expressed in streamflow, and can potentially be delayed

until baseflow conditions, therefore implying interflow and/or short groundwater flow paths. Flow paths and residence times must be considered when estimating recharge and calculating water budgets. These results show that simulated hydrographs compared to isotopic time series highlight important processes and illustrate how a numerical model can be used to compare and discuss geochemical data.

Recharge

Annual groundwater recharge for the Martis Valley watershed varies from year to year based on annual precipitation cycles and temperature fluctuations. The modeled recharge results are based off GSFLOW model simulations of surface water-groundwater interactions throughout the Martis watershed. Governing flow equations solved on a 300 x 300 m cell simulate daily recharge and discharge rates. Recharge varied greatly in time and space, and average values were computed for comparison with previous estimates. The integrated GSFLOW model more realistically distributed recharge over the model domain compared to previous PRMS model simulations of Martis Valley recharge (Rajagopal et al., 2012). PRMS simulations did not account for underlying low-permeability bedrock causing precipitation to be re-distributed down slope as runoff and interflow. The recharge distribution from the GSFLOW simulation corroborates implications from groundwater isotopes and noble gas data (Singleton and Moran, 2010; Segal, 2013).

The measurements of noble gas concentrations and excess air amounts in Martis Valley suggest that the groundwater samples were recharged below the 2050 m elevation contour of the basin, or within the lower 330 m of the watershed (Segal, 2013). The

GSFLOW model does simulate the majority (75%) of recharge occurring below this elevation as well, while much less recharge is simulated in the upper elevation mountain block. The model differs from the geochemical analyses in the emphasis placed on recharge from stream channel and alluvial areas in higher elevations. The geochemical analyses from the Squaw Valley sub-basin (Singleton and Moran, 2010) suggested similar valley recharge dominance, which is confirmed by the model.

As previously stated, groundwater recharge is highly variable in time and space. Clearly, precipitation is the dominant driver of recharge rates, but distribution and timing are functions of temperature, hydrogeology, and possibly antecedent recharge trends from previous years. For example, Figure 26 (page 65) showed variations of spatial recharge over the same three month period during similar water years. Snowmelt timing is likely the principal cause of these variations, but fluctuating vadose zone storage could also attribute to temporal variations of recharge.

Previous recharge estimations for the Martis watershed were largely focused on the central valley area and surrounding tributary streams to the Truckee River, essentially neglecting several significant sub-watershed contributions. The sub-basin analysis reveals that the eastern sub-basins contribute roughly half of total annual groundwater recharge. These contributions are accounted for in the previous recharge estimations.

Hydrologic modeling inherently contains assumptions, generalizations, and uncertainties (i.e. hydrogeologic framework development). The calibration procedure is meant to mitigate potential error, but because so many parameters influence the model, other combinations of parameter values could possible yield acceptable calibration results

(i.e. non-unique results), and potentially effect recharge results. A quantitative assessment of modeling uncertainties is outside the scope of this research.

Conceptual Model

The majority of precipitation in the Martis watershed is received as snow in the upper elevations; however, the valley floor does receive significant precipitation intermittently. Sublimation and evaporation contribute minor losses to the snowpack, while the remaining water permeates shallow soils and interflows over relatively impermeable bedrock into down gradient alluvium and stream channels. A combination of interflow and surface runoff flows towards the valley and infiltrates as mountain front and valley recharge. Stream channels contribute recharge, and groundwater discharge also occurs along intermittent sections of valley streams and the Truckee River. Figure 33 illustrates the conceptualization of precipitation, infiltration, recharge, and discharge in Martis Valley.

In general, the upper elevations of the watershed represent an area of lateral flow (surface runoff and interflow). The interface between mountain block and alluvial fill, in the form of stream channels or valley areas, represents the beginning of the recharge zone. The valley represents a combination of both groundwater recharge and discharge.

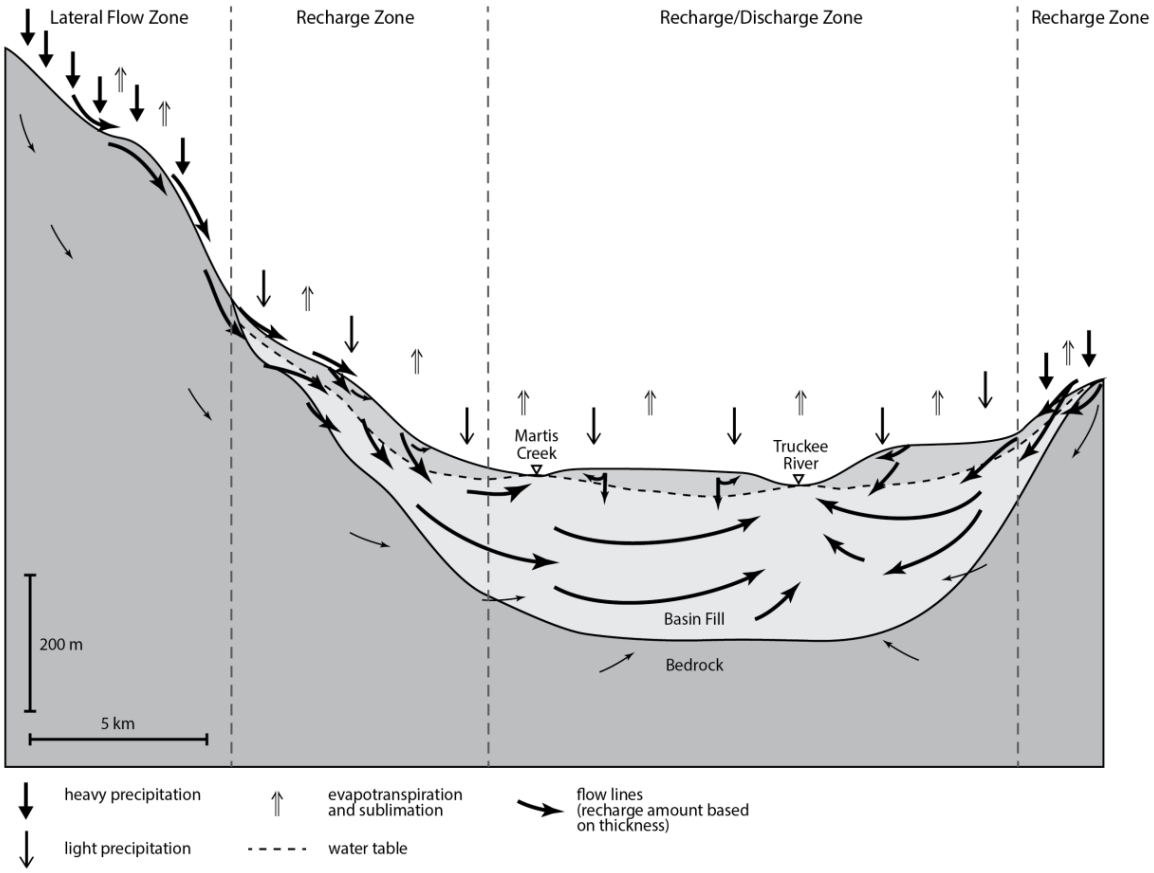

Figure 33: Conceptual model of the Martis Valley basin, emphasizing precipitation in upper elevations, recharge at the mountain front and through the valley floor. Discharge is shown to occur near main stream channels and as sublimation/evapotranspiration. Possible flow through bedrock is indicated, but is negligible compared to magnitudes of flow within other parts of the system.

Recharge source is derived largely from high elevation snowmelt, but occurs in lower elevations as it is re-distributed by interflow and stream channels. Recharged water can remain in the system for a variable amount of time, and will eventually contribute to streamflow as groundwater discharge over a continuum of time scales. This is a function of recharge location, climatic and hydrologic characteristics of the previous and following seasons, and anthropogenic influences such as groundwater pumping.

Convective summer rainstorms are typically characterized as short duration, high intensity, regional storms. This precipitation falls on dry soils and vegetation, and large portions can evapotranspire after a thunderstorm has passed. High deposition rate typical in summer showers will cause Hortonian overland flows that create a short storm event pulse in the hydrograph. Remaining water infiltrates into the shallow sub-surface, with pulses that are mostly confined to the root zone. These rain shower events, however, may increase storage in the unsaturated zone that later reaches the water table, as recharge.

Martis Valley contains large alluvial fans on its southern and south-eastern sides, fanning down from Mt. Pluto and Brockway Summit. These fans are braided with seasonal drainages that act as conduits for spring snowmelt to the valley floor. The mountain block to the north is not as elevated and the alluvial fans are not as large, but a significant amount of groundwater recharge and surface runoff is still contributed by this area. The western side of the watershed consists of several sub-basins that all imitate similar recharge processes of the main valley, and eventually contribute to streamflow and lower elevation recharge. The north-eastern side of the basin contains fewer alluvial fan-basin fill areas, and mainly acts as the discharge section of the study area, where the Truckee River exits the basin.

Summary and Conclusions

Preliminary conceptualizations of Martis Valley watershed interactions were formed in terms of precipitation, recharge, and discharge based on a baseflow analysis. The baseflow analyses suggested that roughly one-sixth of precipitation is reflected as baseflow, and streamflow and baseflow response to precipitation is affected by trends of previous years. Thus, baseflow measurements are not always reflective of recharge of that year. Stable isotope data from LLNL was analyzed and basic relationships between snowmelt, streamflow, and groundwater were observed. Spring streamflow is largely made up of snowmelt, and sublimation effects isotopic evolution of the snowpack.

A novel technique for hydrogeologic framework grid development was formulated that incorporated a combination of data driven hydrostratigraphic interpolation and conceptual understanding of the upper elevation drainages and their connectivity to the basin fill aquifer. This methodology ensured flow continuity within designated hydrogeologic layers and between model grid cells. The hydrogeologic framework was applied to the GSFLOW model, which couples the PRMS and MODFLOW models to run an integrated surface water-groundwater simulation. Sensitivity analyses confirmed a calibrated model, and simulated groundwater head elevations suggested groundwater flow directions generally mimic topography. Simulated hydrographs of snowmelt and streamflow overlaying stable isotope data provided observations of snowmelt isotopic evolution and timing, as well as timing and expression of snowmelt in valley streamflow. These results highlight the compatibility of hydrologic modeling with geochemical analyses.

Average annual and monthly recharge locations and amounts were determined from the GSFLOW simulation. Annual recharge for the entire watershed was estimated to be approximately 57,000 ac-ft, with roughly 75% occurring below 2050 m. The recharge locations confirm the geochemical implications of substantial low elevation valley recharge, but also suggest high elevation recharge occurring along stream channel and upland valley areas. Very little recharge occurs in the upper elevation mountain block. Intraseasonal and interseasonal variations were observed, but recharge was consistently heaviest in the spring months throughout the watershed, while residual and less significant valley and stream channel recharge continued through the water year. Average recharge efficiency for areas below 1800 m was estimated to be 30%. For areas between 1800 m and 2050 m, recharge efficiency was calculated to be 17%, and estimated to be 9% above 2050 m. Total annual estimations of groundwater recharge are higher than previous methods, but included several sub-watersheds not previously considered.

Groundwater recharge is an essential variable to understand when assessing the governing hydrologic processes of a watershed and attempting to predict future scenarios. The more limited the water resource within a basin, the more detailed an understanding is required for efficient management of the hydrologic system. The Truckee River Basin is limited in its water resources and depends heavily on Martis Valley groundwater contributions. The recharge locations, timing, and magnitudes gathered from this research provide interesting details that may be considered by water resource and land managers of the Truckee River Basin.

References

Ajami, H., P. A. Troch, T. Maddock III, T. Meixner, and C. Eastoe (2011), Quantifying mountain block recharge by means of catchment-scale storage-discharge relationships, Water Resour. Res., 47, W04504, doi:10.1029/2010WR009598.

Bauer, T.M., D. Shaw, P. Selsky (2013), Martis Valley Groundwater Management Plan Nevada and Placer Counties, California: Draft. Brown and Caldwell; Balance Hydrologics, Inc.; Prepared for TDPUD, Placer County Water agency, Northstar Community Services District. 1/10/2013.

Bedrosian, Paul A., B.L. Burton, M.H. Powers, B.J. Minsley, J.D. Phillips, and L.E. Hunter (2012), Geophysical investigations of geology and structure at the Martis Creek Dam, Truckee, California, US Army Research. Paper 181.

Bottomley, D.J., D.Craig, and L.M. Johnston (1986), Oxygen-18 studies of snowmelt runoff in a small precambrian shield watershed: implications for streamwater acidification in acid sensitive terrain. *J. Hydrol.* 88: 213-234.

California Department of Water Resources (2006), Martis Valley Groundwater Basin. California's Groundwater, Bulletin 118. 1/20/2006

Carling, G.T., A.L. Mayo, D. Tingley, J. Bruthans (2012), Mechanisms, timing, and rates of arid region mountain front recharge, Journal of Hydrology 428–429 (2012) 15–31.

Cey, B. D., G. B. Hudson, J. E. Moran, and B. R. Scanlon (2008), Impact of artificial recharge on dissolved noble gases in groundwater in California, Environ. Sci. Technol., 42(4), 1017‐1023, doi:10.1021/es0706044.

Cey, B. D., G. B. Hudson, J. E. Moran, and B. R. Scanlon (2009), Evaluation of noble gas recharge temperatures in a shallow unconfined aquifer, Ground Water, 47(5), 646‐659, doi:10.1111/j.1745-6584.2009.00562.x.

Clark, I.D. and P. Fritz (1997), Environmental Isotopes in Hydrogeology, 328pp. CRC Press/Lewis Publishers, Boca Raton, FL.

Conlon T.D., K.C. Wozniak, D. Woodcock, N.B. Herrera, B.J. Fisher, D.S. Morgan, K.K. Lee, and S.R. Hinkle (2005), Ground-Water Hydrology of the Willamette Basin, Oregon: U.S. Geological Survey Scientific Investigations Report 2005–5168, 83 p.

Daly, C., R. P. Neilson, and D. L. Phillips (1994), A statistical-topographic model for mapping climatological precipitation over mountainous terrain. Journal of Applied Meteorology 33, 140-158.

Daly, C., M. Halbleib, J.I. Smith, W.P. Gibson, M.K. Doggett, G.H. Taylor, J. Curtis, and P.P. Pasteris (2008), Physiographically sensitive mapping of climatological temperature and precipitation across the conterminous United States, International Journal of Climatology, DOI: 10.1002/joc.1688

Epstein, B.J. (2004), Development and uncertainty analysis of an empirical recharge prediction model for Nevada's desert basins, Master's Thesis, University of Nevada, Reno.

Ferguson, I. M., and R. M. Maxwell (2010), Role of groundwater in watershed response and land surface feedbacks under climate change, Water Resour. Res., 46, W00F02, doi:10.1029/2009WR008616.

Fetter, C.W. (2001), Applied Hydrology – 4th ed. Prentice Hall Inc., New Jersey, 598 p.

Fritz, P., J.A. Cherry, K.V. Weyer, and M.G. Sklash (1976), Runoff analysis using environmental isotope and major ions. In Interpretation of Environmental Isotope and Hydrochemical Data in Groundwater Hydrology. IAEA, Vienna. pp. 111-130.

Harbaugh, A.W. (2005), MODFLOW-2005, the U.S. Geological Survey modular ground-water model-the Ground-Water Flow Process: U.S. Geological Survey Techniques and Methods 6-A16, variously paginated.

Harbaugh, A.W., E.R. Banta, M.C. Hill, and M.G. McDonald (2000), MODFLOW-2000, the U.S. Geological Survey modular ground-water model-modularization concepts and the ground-water flow process: U.S. Geological Survey Open-File Report 00-92, 121 p.

Harbaugh, A.W., and M.G. McDonald (1996), User's documentation for MODFLOW-96, and update to the U.S. Geological Survey modular finite-difference ground-water flow model: U.S. Geological Survey Open-File Report 96-485, 56 p.

Hardman, G. (1936), Nevada precipitation and acreages of land by rainfall zones: University of Nevada, Reno, Agricultural Experiment Station Report, 10 p.

Hardman, G., V. Kral, and J. Haffey (1965), Nevada Precipitation Map. *in*. Nevada Agricultural Experiment Station.

Healy, R.W. (2010), Estimating Groundwater Recharge, Cambridge: Cambridge University Press. 264 p.

Herrmann, A., J. Koll, P. Maloszewski, W. Rauert, and W. Stichler (1986), Water balance studies in a small catchment on paleozoic rock using environmental isotope tracer techniques. IAHS Publ. 156: 111-124.

Huntington, J. L., and R. G. Niswonger (2012), Role of surface-water and groundwater interactions on projected summertime streamflow in snow dominated regions: An integrated modeling approach, Water Resour. Res., 48, W11524, doi:10.1029/ 2012WR012319.

Huntington, J.L., R.G. Niswonger, S. Rajagopal, Y. Zhang, M. Gardner, C.G. Morton, D.M. Reeves, D. McGraw, G.M. Pohll (2013), Integrated Hydrologic Modeling of Lake Tahoe and Martis Valley Mountain Block and Alluvial Systems, Nevada and California, Desert Research Institute, 5 p.

Jeton, A. E., and D. K. Maurer (2007), Precipitation and runoff simulations of the Carson Range and Pine Nut Mountains, and updated estimates of ground-water inflow and the ground-water budget for basin-fill aquifers of Carson Valley, Douglas County, Nevada, and Alpine County, California, U.S. Geol. Surv. Sci. Invest. Rep. 2007–5205, 56p.

Jeton, A. E., and D. K. Maurer (2011), Precipitation and runoff simulations of select perennial and ephemeral watersheds in the middle Carson River basin, Eagle, Dayton, and Churchill Valleys, west-central Nevada, U.S. Geol. Surv. Sci. Invest. Rep. 2011–5066, 44p.

Kennedy, V.C., C. Kendall, G.W. Zellweger, T.A. Wynman, and R.J. Avanzino (1986) Determination of the components of stormflow using water chemistry and environmental isotopes, Mattole River basin, California. J. Hydrol. 84: 107-140.

Kirchner, J. W. (2009), Catchments as simple dynamical systems: Catchment characterization, rainfall-runoff modeling, and doing hydrology backward, Water Resour. Res., 45, W02429, doi:10.1029/2008WR006912.

Kollet, S. J., and R. M. Maxwell (2006), Integrated surface-groundwater flow modeling: A free surface overland flow boundary condition in a parallel groundwater flow model, Adv. Water Resour., 29(7), 945– 958.

Kollet, S. J., and R. M. Maxwell (2008), Capturing the influence of groundwater dynamics on land surface processes using an integrated, distributed watershed model, Water Resour. Res., 44, W02402, doi:10.1029/2007WR006004.

Lamb, R. (1996), Distributed hydrological prediction using generalized TOPMODEL concepts, Ph.D. thesis, Lancaster University, Lancaster, U.K.

Lamb R. and K. Beven (1997), Using interactive recession curve analysis to specify a general catchment storage model, Hydrology and Earth System Sciences, 1, 101–113.

Leavesley, G. H., R.W. Lichty, B.M. Troutman, and L.G. Saindon (1983), Precipitation-Runoff Modeling System: User's Manual. U.S. Geological Survey, MS 412, Denver Federal Center, Box 25046, Lakewood, CO 80225. Water Resources Investigation Report 83-4238

Leavesley, G. H. and L.G. Stannard (1995), The Precipitation-Runoff Modeling System - PRMS. Water Resources Division, U.S. Geological Survey, MS 412, Denver Federal Center, Box 25046, Lakewood, CO 80225, USA. Singh, V. P. Computer models of watershed hydrology. 1995 pp. 281-310

Leibundgut C., P. Malozewski, and C. Külls (2009), Tracers in Hydrology, John Wiley & Sons: Chichester.

Manning, A. H., and J. S. Caine (2007), Groundwater noble gas, age, and temperature signatures in an Alpine watershed: Valuable tools in conceptual model development, Water Resour. Res., 43, W04404, doi:10.1029/2006WR005349.

Manning, A. H., and D. K. Solomon (2005), An integrated environmental tracer approach to characterizing groundwater circulation in a mountain block, Water Resour. Res., 41, W12412, doi:10.1029/2005WR004178.

Manning, A. H., and D. K. Solomon (2003), Using noble gases to investigate mountain-front recharge, Journal of Hydrology, 275 (2003) 194–207. Elsevier Science B.V.

Markstrom, S. L., R. G. Niswonger, R. S. Regan, D. E. Prudic, and P. M. Barlow (2008), GSFLOW-Coupled Ground-water and Surface-water FLOW model based on the integration of the Precipitation-Runoff Modeling System (PRMS) and the Modular Ground-Water Flow Model (MODFLOW-2005), U.S. Geological Survey Techniques and Methods 6-D1, 240 p.

Mau, D. P. and T. C. Winter (1997), Estimating Groundwater Recharge from Streamfiow Hydrographs for a Small Mountain Watershed in a Temperate Humid Climate, New Hampshire, USA. Groundwater 35(2):291-304.

Maxey, G. B., and T. E. Eakin (1949), Ground water in White River Valley, White Pine, Nye, and Lincoln Counties, Nevada. No. 8, State of Nevada Office of the State Engineer prepared in cooperation with the United State Department of the Interior Geological Survey, Carson City, Nevada.

Meyboom, P. (1961), Estimating Ground-Water Recharge from Stream Hydrographs, Journal of Geophysical Resources, vol. 66, pp. 1203–1214.

McDonald, M.G., and A.W. Harbaugh (1988), A modular three-dimensional finite-difference ground-water flow model: U.S. Geological Survey Techniques of Water-Resources Investigations, Book 6, Chapter A-1, 586 p.

McNamara, J.P., D.L. Kane, and L. D. Hinzman (1997), Hydrograph separations in an Arctic watershed using mixing model and graphical techniques. Water and Environmental Research Center, University of Alaska Fairbanks. Paper number 97WR01033, 13 p.

Niblach, R. L. (1988) ,Geophysical Investigations of the Ward Valley Aquifer, Lake Tahoe, CA. Master's Thesis.

Nichols, W. D. (2000), Regional Ground-Water Evapotranspiration and Ground-Water Budgets. Professional Paper 1628, United States Geologic Survey, Reston, Virginia.

Niswonger, R.G. and D.E. Prudic (2005), Documentation of the Streamflow-Routing (SFR2) Package to include unsaturated flow beneath streams -- a modification to SFR1: U.S. Geological Techniques and Methods Book 6, Chapter A13, 47 p.

Niswonger, R.G., D.E. Prudic, and R.S. Regan (2006), Documentation of the Unsaturated-Zone Flow (UZF1) Package for modeling unsaturated flow between the land surface and the water table with MODFLOW-2005: U.S. Geological Techniques and Methods Book 6, Chapter A19, 62 p.

Niswonger, R.G., S. Panday, and M. Ibaraki (2011), MODFLOW-NWT, A Newton formulation for MODFLOW-2005: U.S. Geological Survey Techniques and Methods, 6-A37, 44 p.

Pollock, D.W. (2012), User Guide for MODPATH Version 6—A Particle-Tracking Model for MODFLOW: U.S. Geological Survey Techniques and Methods 6–A41, 58 p.

Posavec, K., J. Parlov, and Z. Nakic (2010), Fully Automated Objective-Based Method for Master Recession Curve Separation, Groundwater, Vol. 48, No. 4 p. 598-603.

Rademacher, L. K., J. F. Clark, G. B. Hudson, D. C. Erman, and N. A. Erman (2001), Chemical evolution of shallow groundwater as recorded by springs, Sagehen Basin, Nevada County, California, Chem. Geol., 179, 37– 51.

Rademacher, L. K., J. F. Clark, D. W. Clow, and G. B. Hudson (2005), Old groundwater influence on stream hydrochemistry and catchment response times in a small Sierra Nevada catchment: Sagehen Creek, California, Water Resour. Res., 41, W02004, doi:10.1029/2003WR002805.

Rajagopal, S., D.M. Reeves, J. Huntington, and G. Pohll (2012), Desert Research Institute Technical Note to PCWA: Estimates of Ground Water Recharge in the Martis Valley Ground Water Basin: prepared for PCWA, 11 p..

Rodhe, A. (1984), Groundwater contribution to streamflow in Swedish forested till soil as estimated by oxygen-18. Isotope Hydrology, IAEA, Vienna: pp. 55-66.

Rorabaugh, M. I. (1964), Estimating Changes in Bank Storage and Groundwater Contribution to Streamflow. International Association of Scientific Hydrology 63:432-441.

Rose, T.P. and M.L. Davisson (2002), Isotopic and Geochemical Evidence for Holocene-age Groundwater in Regional Flow Systems of South-central Nevada, Ch. 8 of Hydrologic Resource Management Program and Underground Test Area Project FY200 Progress Report. LLNL, June 2002, UCRL-ID-145167 p. 99-135.

Rutledge, A. T. (1993), Computer Programs for Describing the Recession of Groundwater Discharge and for Estimating Mean Groundwater Recharge and Discharge from Streamflow Records. U.S. Geological Survey Water Resources Investigations Report 93-4121,45 pp.

Singleton, M. J., and J. E. Moran (2010), Dissolved noble gas and isotopic tracers reveal vulnerability of groundwater in a small, high‐elevation catchment to predicted climate changes, Water Resour. Res., 46, W00F06, doi:10.1029/2009WR008718.

Segal, D. (2013), Dissolved Gases and Isotopes as Tools for Aquifer Characterization in Martis Valley, Master's Thesis, California State University East Bay, Hayward, CA.

Sklash, M.G. and R.N. Farvolden (1979), The role of groundwater in storm runoff. Journal of Hydrology. 43: 45-65.

Somorowska, U. (2004), Inferring changes in dynamic groundwater storage from recession curve analysis of discharge data. Micellanea Geographica, WARSZAWA 2004, Vol. 11, 8 p.

Sylvester, A.G., W.S. Wise, J.T. Hastings, and L.A. Moyer (2007, updated 2012), Geologic Map of the North Lake Tahoe-Donner Pass Region, Northern Sierra Nevada, California. California Geological Survey, California Dept. of Conservation.

Sulis, M., C. Paniconi, C. Rivard, R. Harvey, and D. Chaumont (2011), Assessment of climate change impacts at the catchment scale with a detailed hydrological model of surface-subsurface interactions and comparison with a land surface model, Water Resour. Res., 47, W01513, doi:10.1029/2010WR009167.

Thiros, S.A. and A.H. Manning (2001), Quality of Ground Water used for Public Supply in Salt Lake Valley, Salt Lake County, Utah, 2001. U.S. Geological Survey, Water Resources Investigation Report 03-4325. National Water-Quality Assessment Program

Thodal,C. E. (1992), Geophysical, Hydrogeologic, and Water-Quality Data for Area Tributary to Lake Tahoe in Douglas County and Carson City NV, through 1987. Open-file Report 89-263. USGS. 32 p.

Thodal,C. E. (1997), Hydrogeology of Lake Tahoe Basin, California and Nevada, and Results

of a Ground-Water Quality Monitoring Network, Water Years 1990-1992. Water-Resources Investigations Report 97-4072. USGS. 53 p.

Turner, J.V., D.K. MacPherson, and R.A. Stokes (1987), The mechanisms of catchment flow processes using natural variations in deuterium and oxygen-18. J. Hydrol. 94: 143-162.

U.S. Department of Interior (2003), Water 2025: Preventing Crises and Conflict in the West, Office of the Secretary, News for immediate release May 2, 2003.

Wahi A.K., J.F. Hogan, B. Ekwurzel, M.N. Baillie, and C.J. Eastoe (2008), Geochemical quantification of semiarid mountain recharge. Ground Water. ;46:414–425.

Watson , P., P. Sinclair, and R. Waggoner (1976), Quantitative evaluation of a method for estimating recharge to the desert basins of Nevada, Journal of Hydrology, Volume 31, Issues 3–4, Pages 335-357, ISSN 0022-1694.